

# High-energy cosmic rays at LOFAR.



LORA Scintillator



university of  
groningen

Olaf Scholten

kvi - center for advanced  
radiation technology

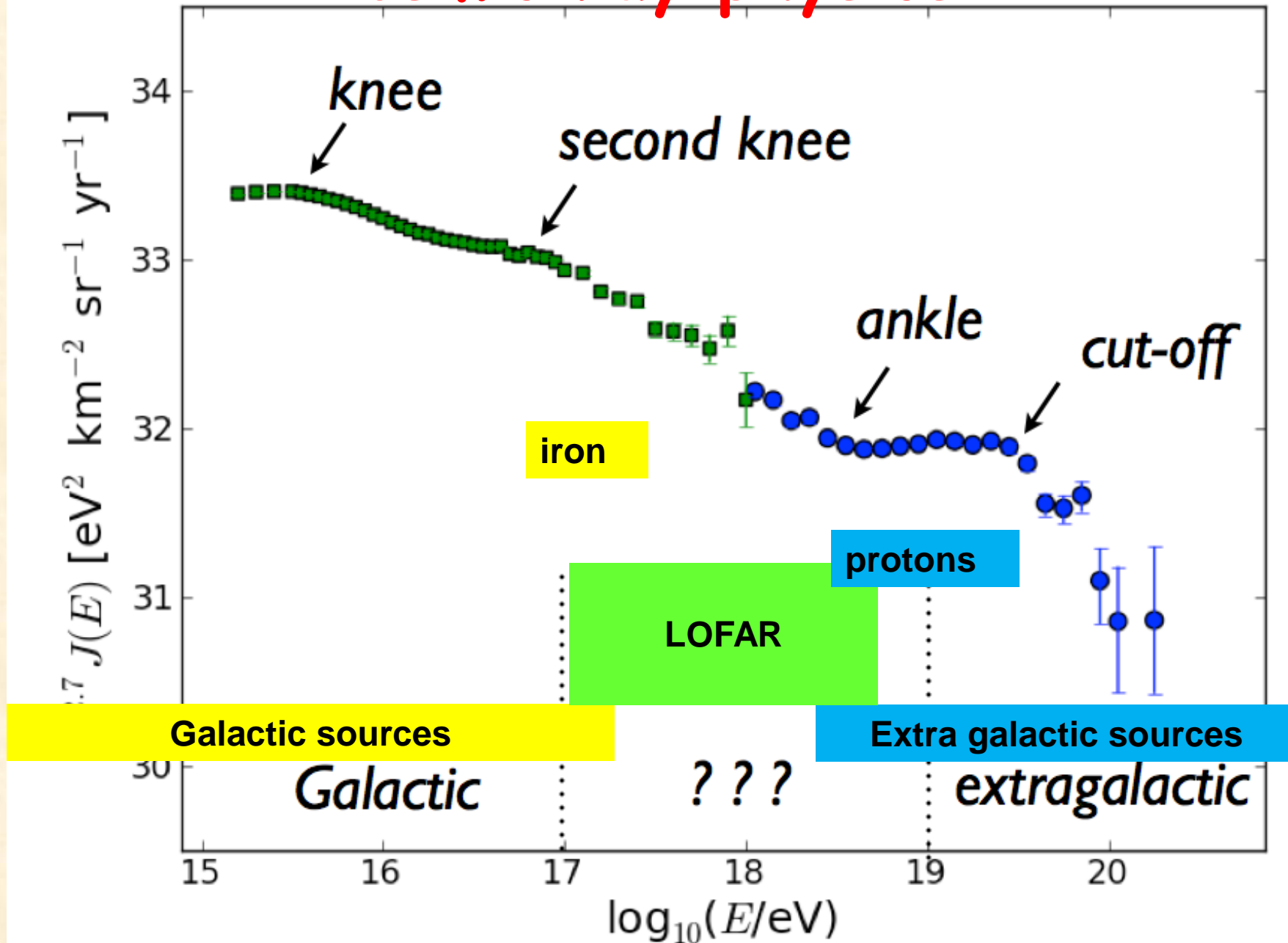
TBB

*LOFAR Cosmic Ray KSP & Cosmic Lightning Project*

A. Bonardi, S. Buitink, A. Corstanje, J.E. Enriquez, H. Falcke, J.R. Hörandel, T. Karskens, M. Krause, P. Mitra, K. Mulrey,  
B.A. Nelles, J.P. Rachen, L. Rossetto, P. Schellart, O. Scholten, S. Thoudam, T.N.G. Trinh , S. ter Veen, T. Winchen

# Cosmic ray physics:

Presentation  
by  
Stijn Buitink

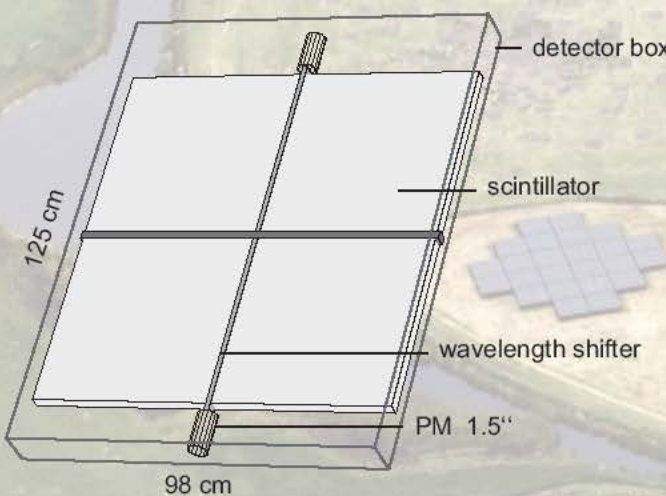


# LOFAR Radboud Air Shower Array - LORA

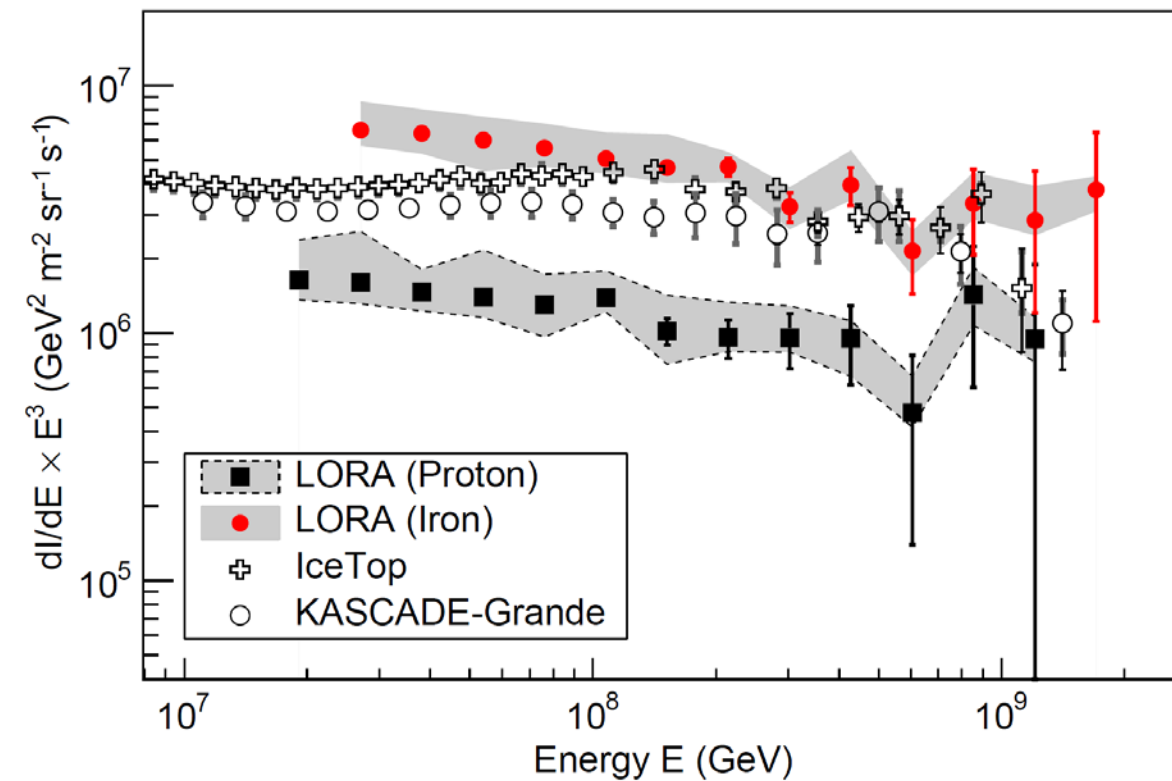
20 scintillator units  
(~1 m<sup>2</sup> each)  
in LOFAR core

→ provide

- properties of EAS
- and trigger



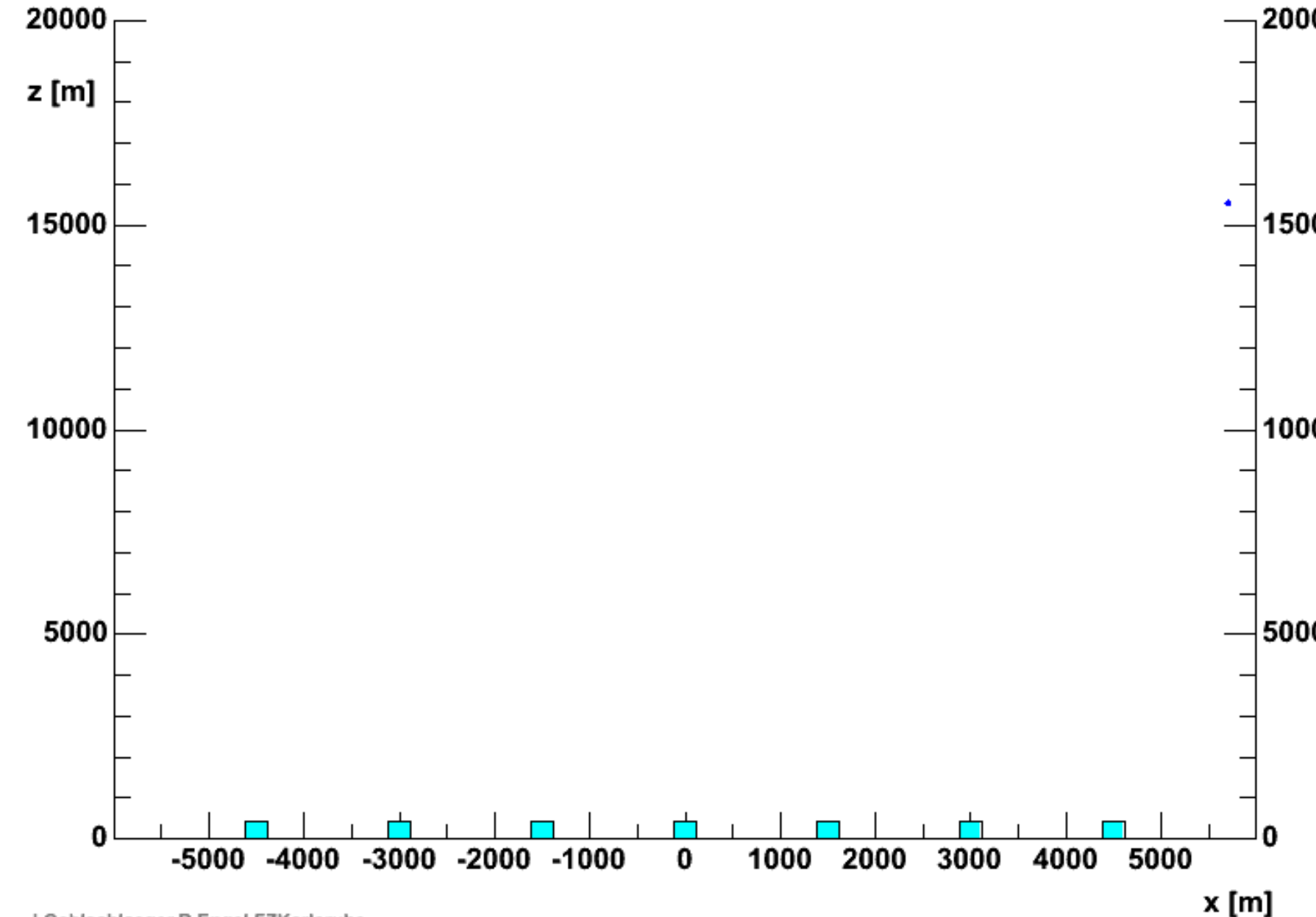
S. Thoudam et al, Astroparticle Physics 73 (2016) 34



hadrons muons electrs neutrals

Proton  $10^{15}$  eV

15514



Air shower,  
side view

# Multiple emission mechanisms

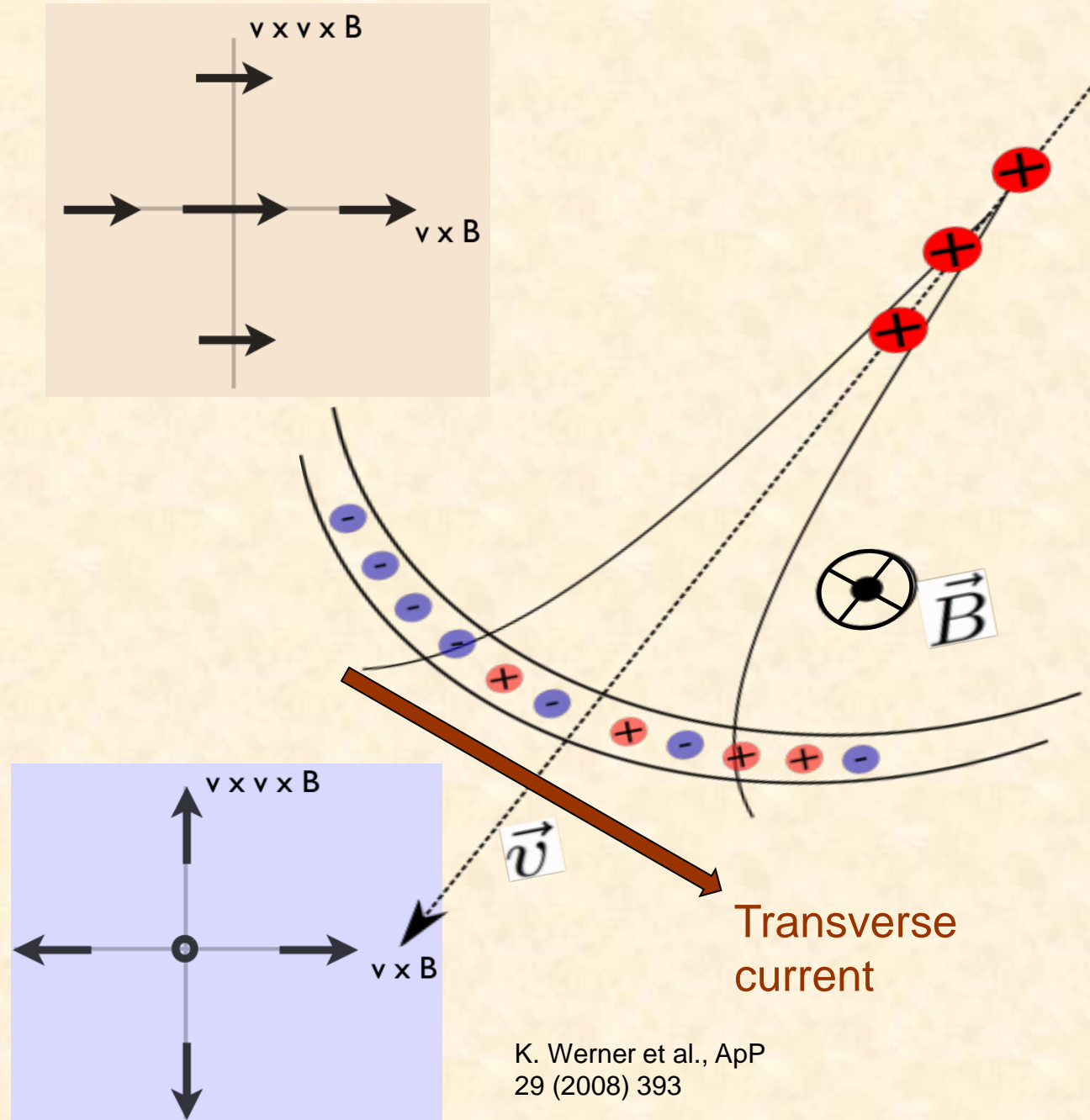
## # Geomagnetic:

- Electrons & positrons have transverse drift, induced by geomagnetic field.
- Linearly polarized, Unidirectional along  $v \times B$

## # Charge excess:

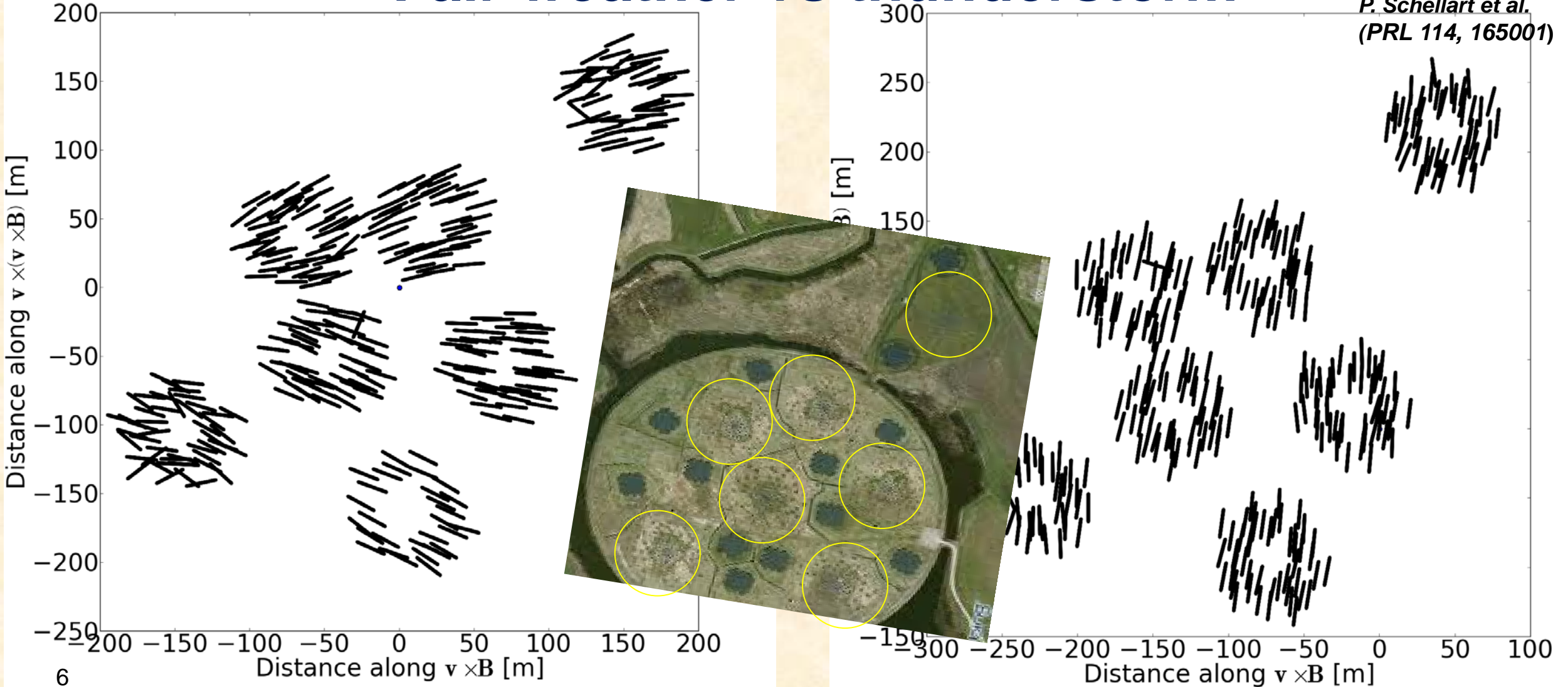
- Negative charge buildup at shower front.
- Linearly polarized, Radially from shower axis

The full signal:  $\vec{E} = \vec{E}_G + \vec{E}_C$  modified by Time-compression effects.



# Observations: polarization footprint

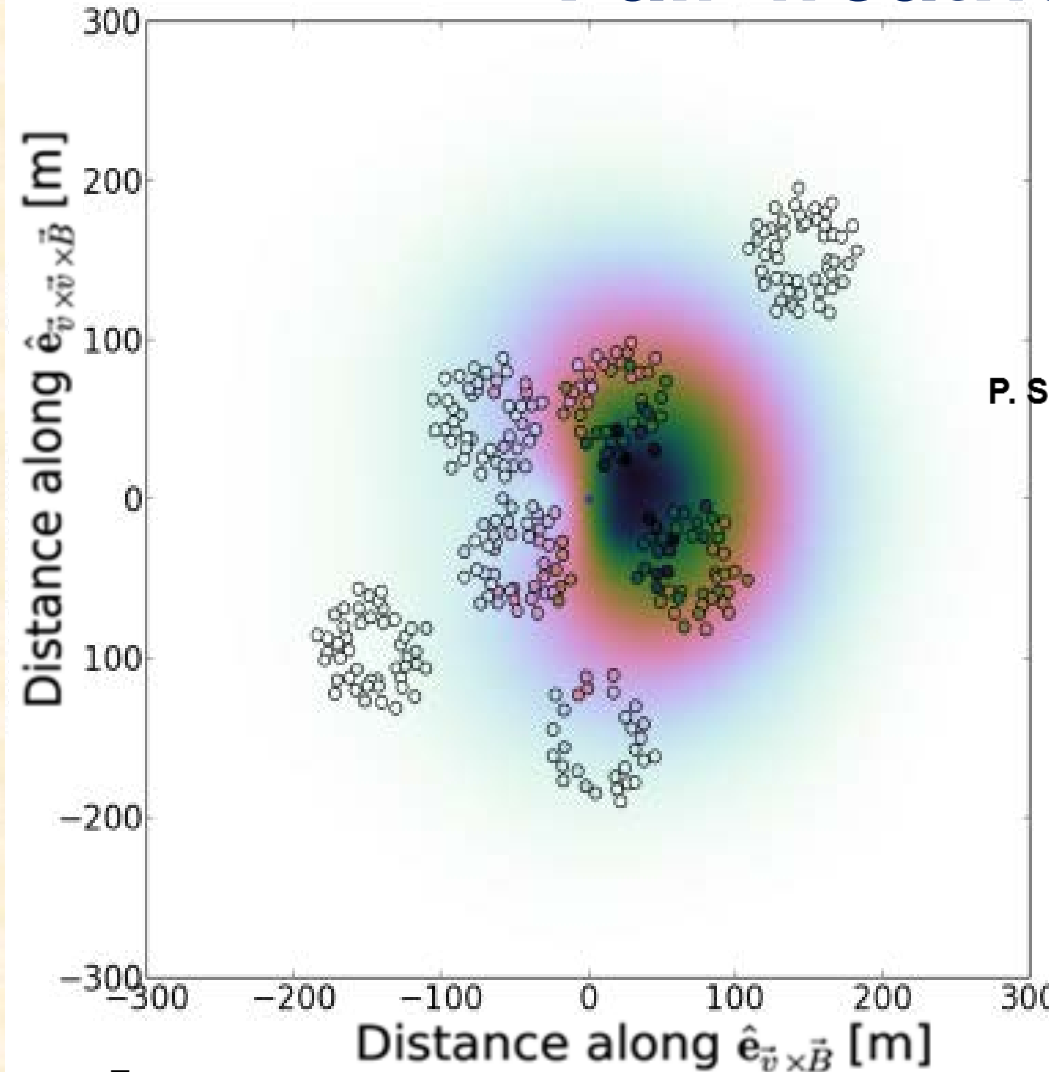
## Fair weather vs thunderstorm



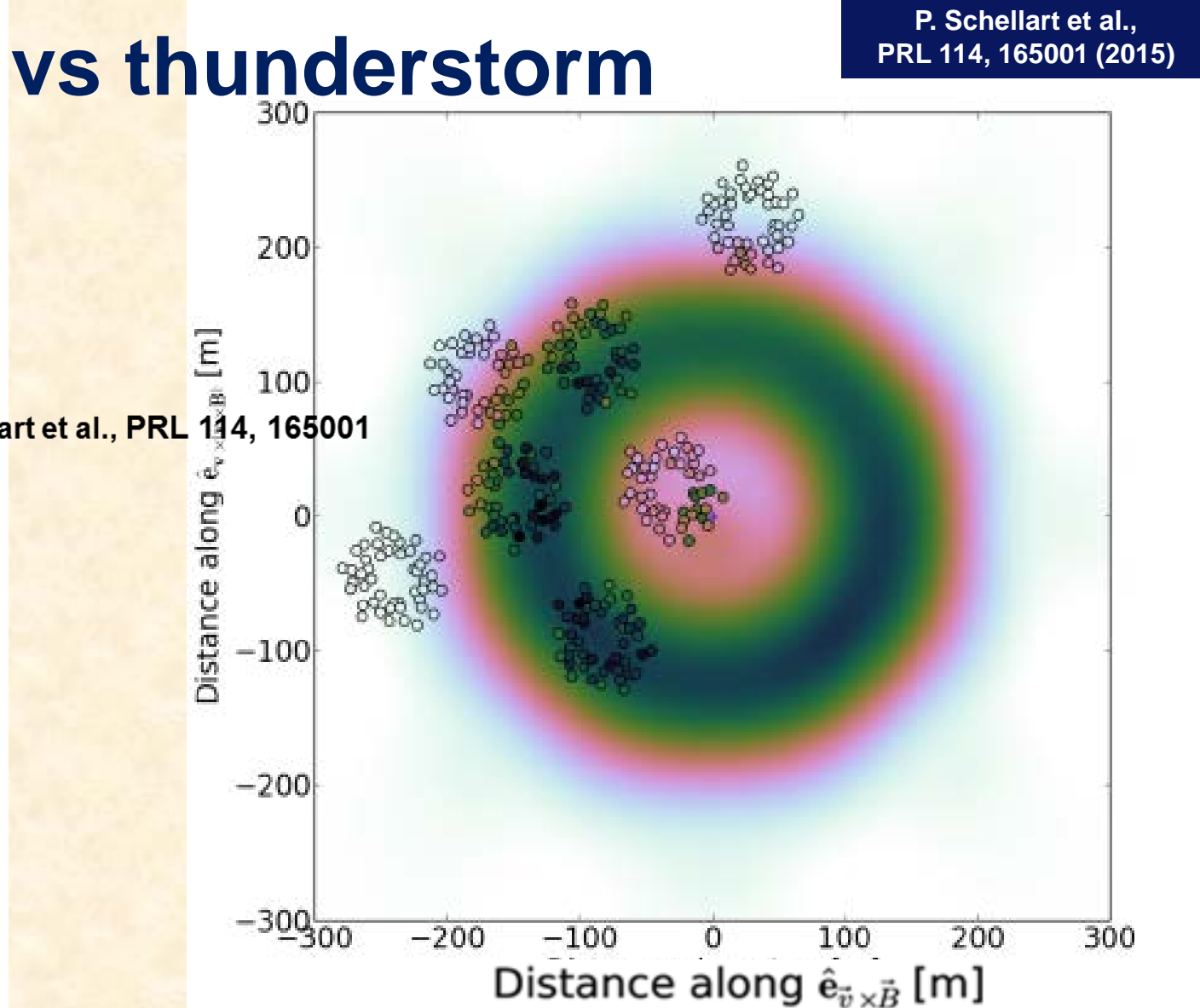
# Observations: intensity footprint

S. Buitink et al.  
PRD 90, 082003 (2014)

## Fair weather vs thunderstorm

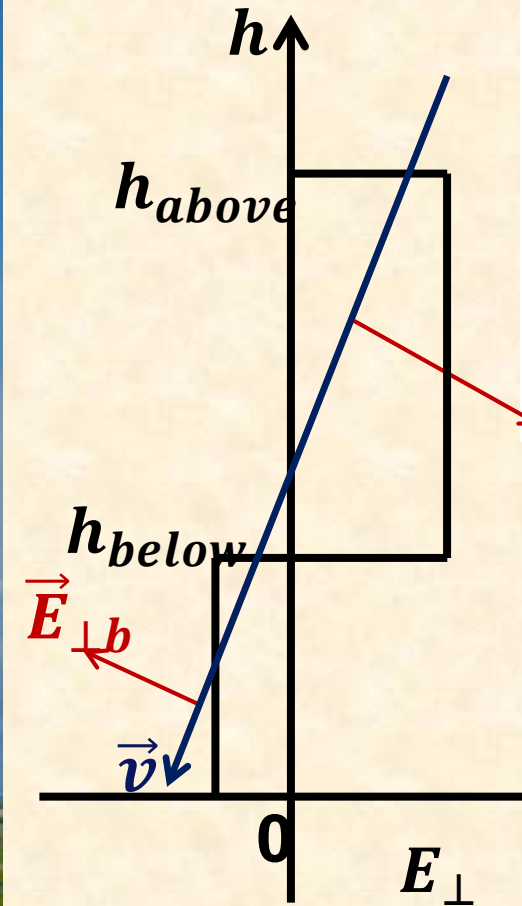
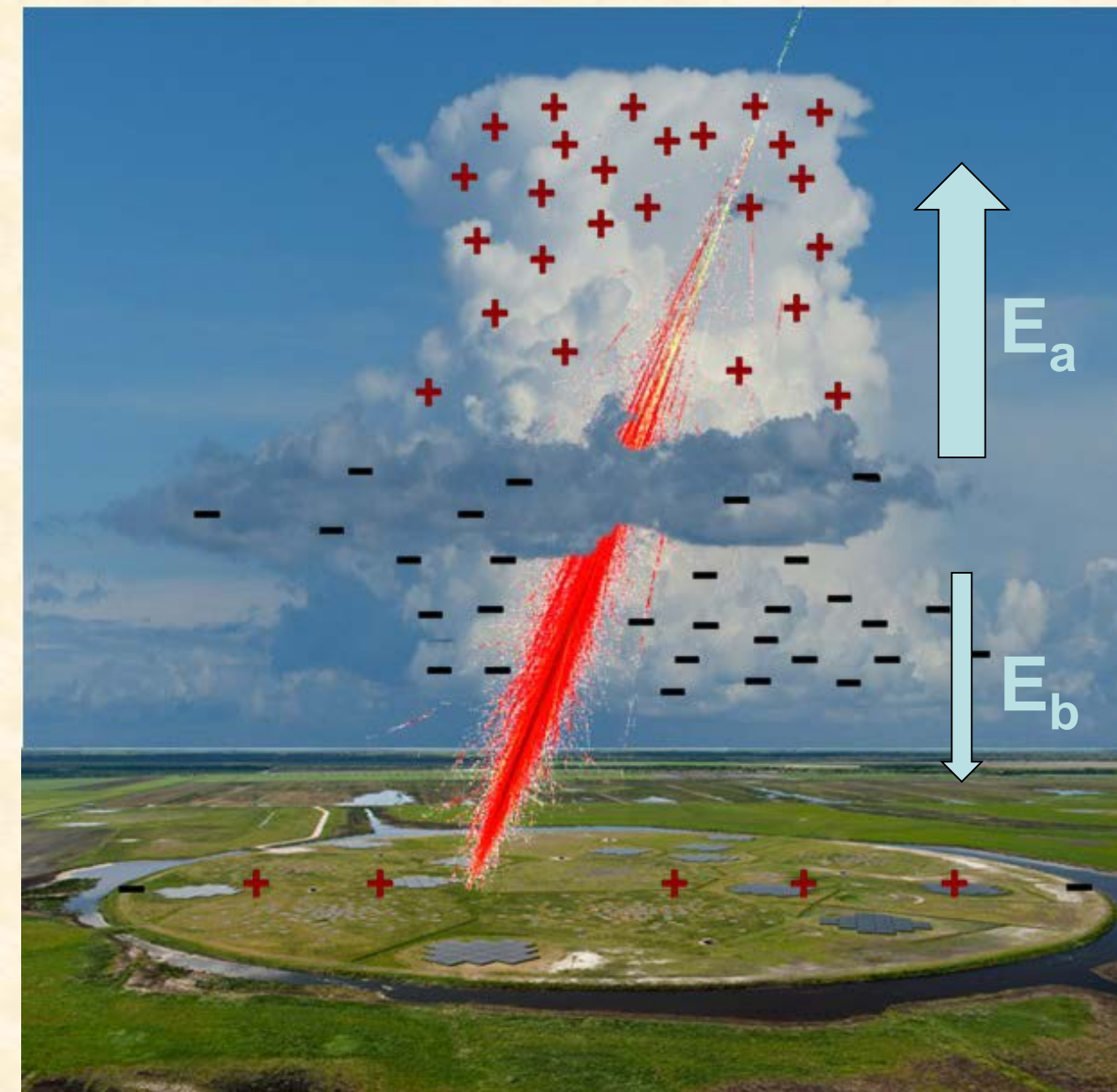


P. Schellart et al., PRL 114, 165001

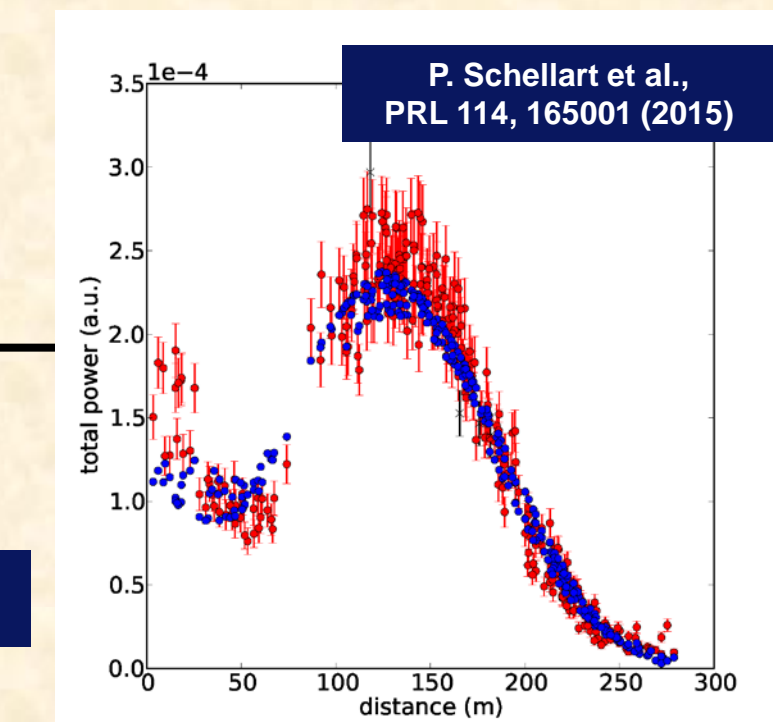
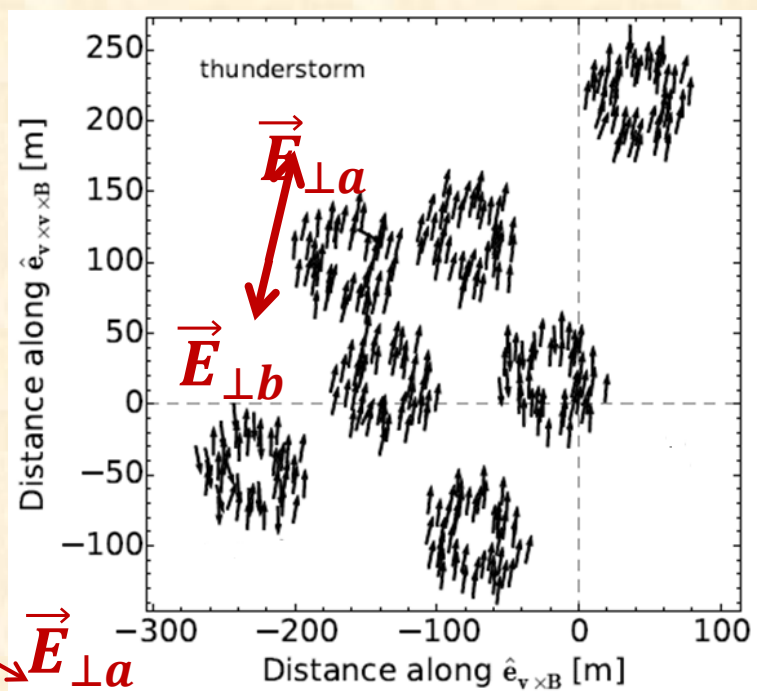


P. Schellart et al.,  
PRL 114, 165001 (2015)

# Structure E-fields



T.N.G. Trinh et al.,  
Phys Rev D 93 (2016) 023003



# Full polarization, Stokes

$$I = \frac{1}{n} \sum_0^{n-1} \left( |\mathcal{E}|_{i, \vec{v} \times \vec{B}}^2 + |\mathcal{E}|_{i, \vec{v} \times \vec{v} \times \vec{B}}^2 \right)$$

$$Q = \frac{1}{n} \sum_0^{n-1} \left( |\mathcal{E}|_{i, \vec{v} \times \vec{B}}^2 - |\mathcal{E}|_{i, \vec{v} \times \vec{v} \times \vec{B}}^2 \right)$$

$$U + iV = \frac{2}{n} \sum_0^{n-1} \left( \mathcal{E}_{i, \vec{v} \times \vec{B}} \mathcal{E}_{i, \vec{v} \times \vec{v} \times \vec{B}}^* \right) .$$

Stokes parameters: I, Q, U, V

Linear polarization angle:  $2\phi = \text{atan}(U/Q)$

NEW: Circular polarization = V/I

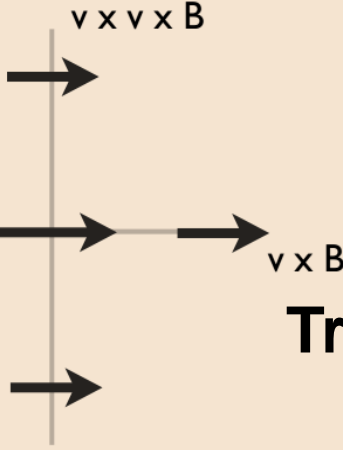
**Interesting results:**

- **Fair weather:**  
**confirmation of emission mechanisms**
- **Thunderstorm:**  
**Finite circular pol. near core due to changing atmospheric E-field**

Presentation

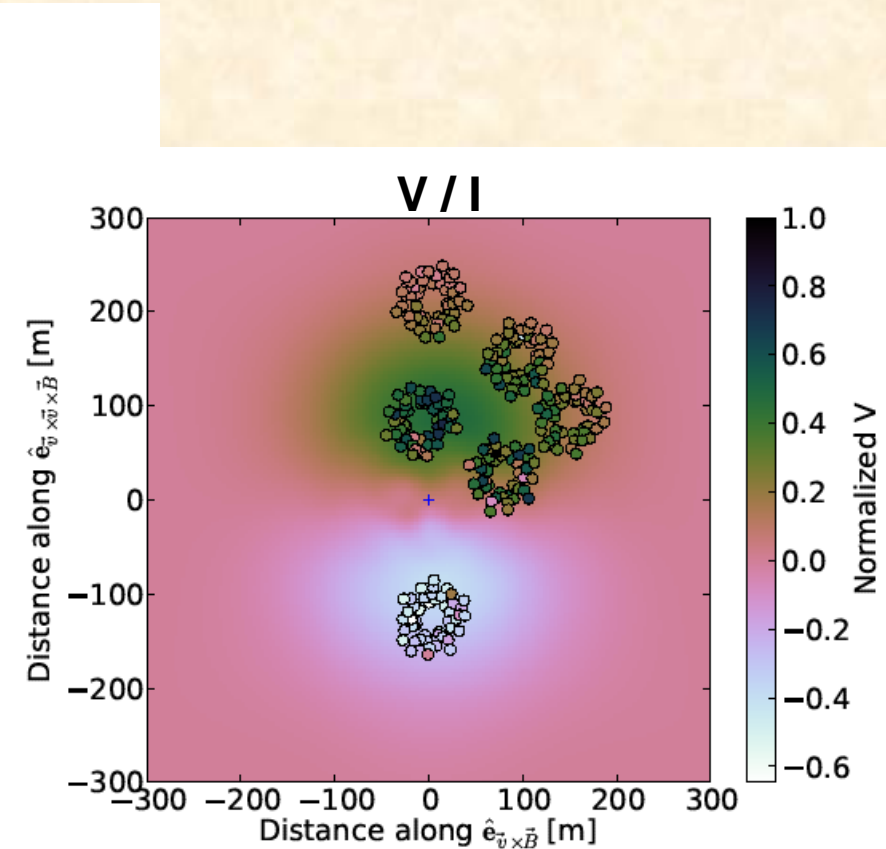
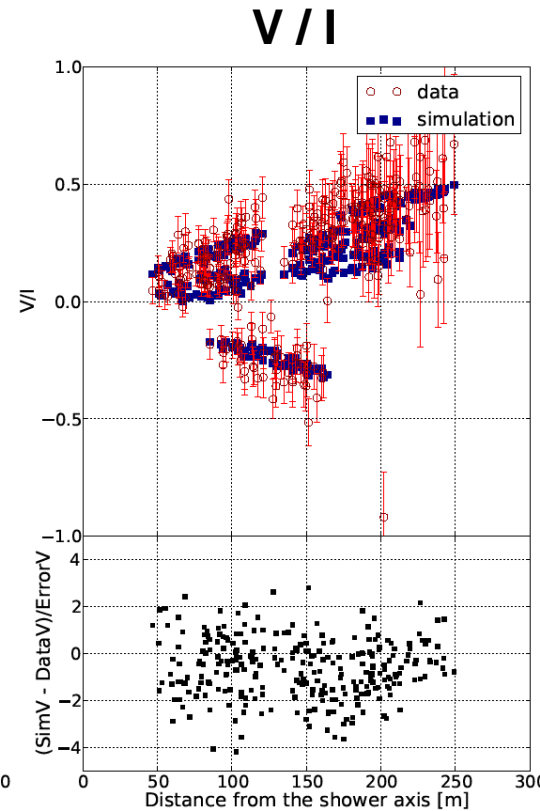
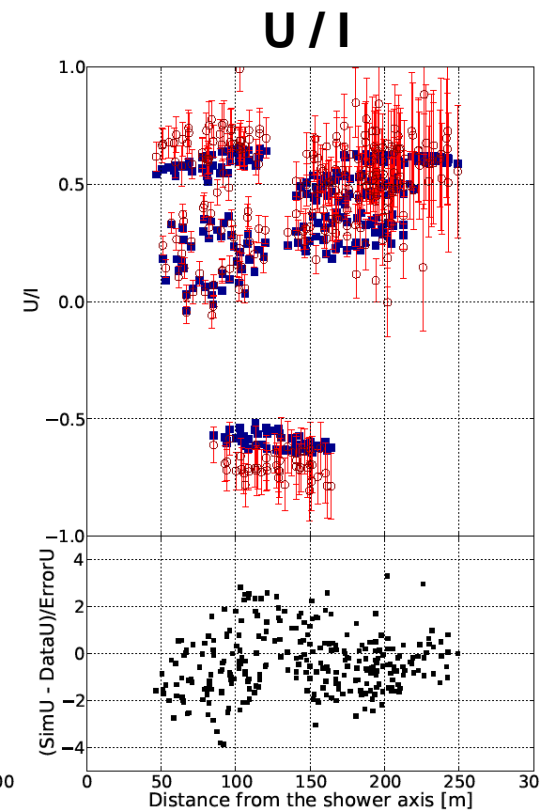
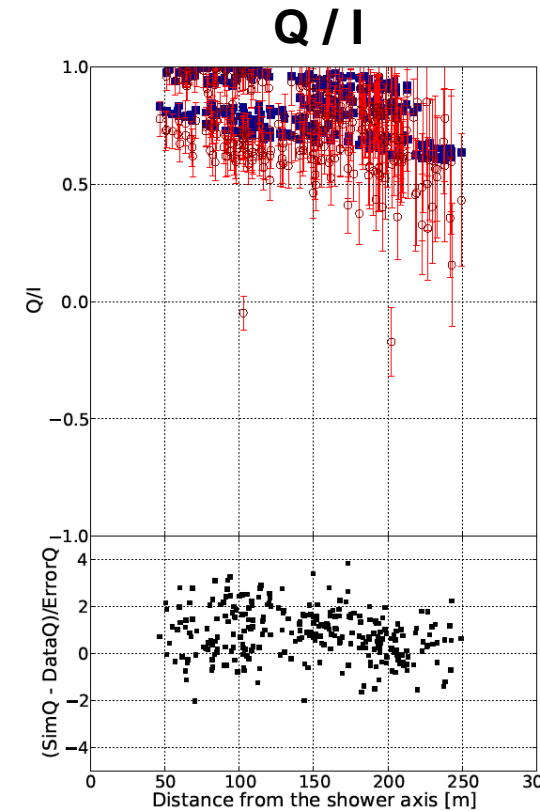
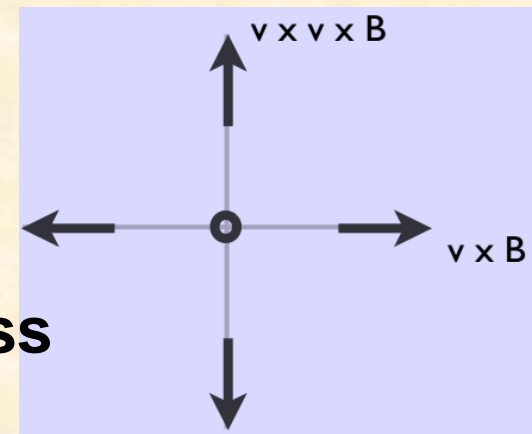
by

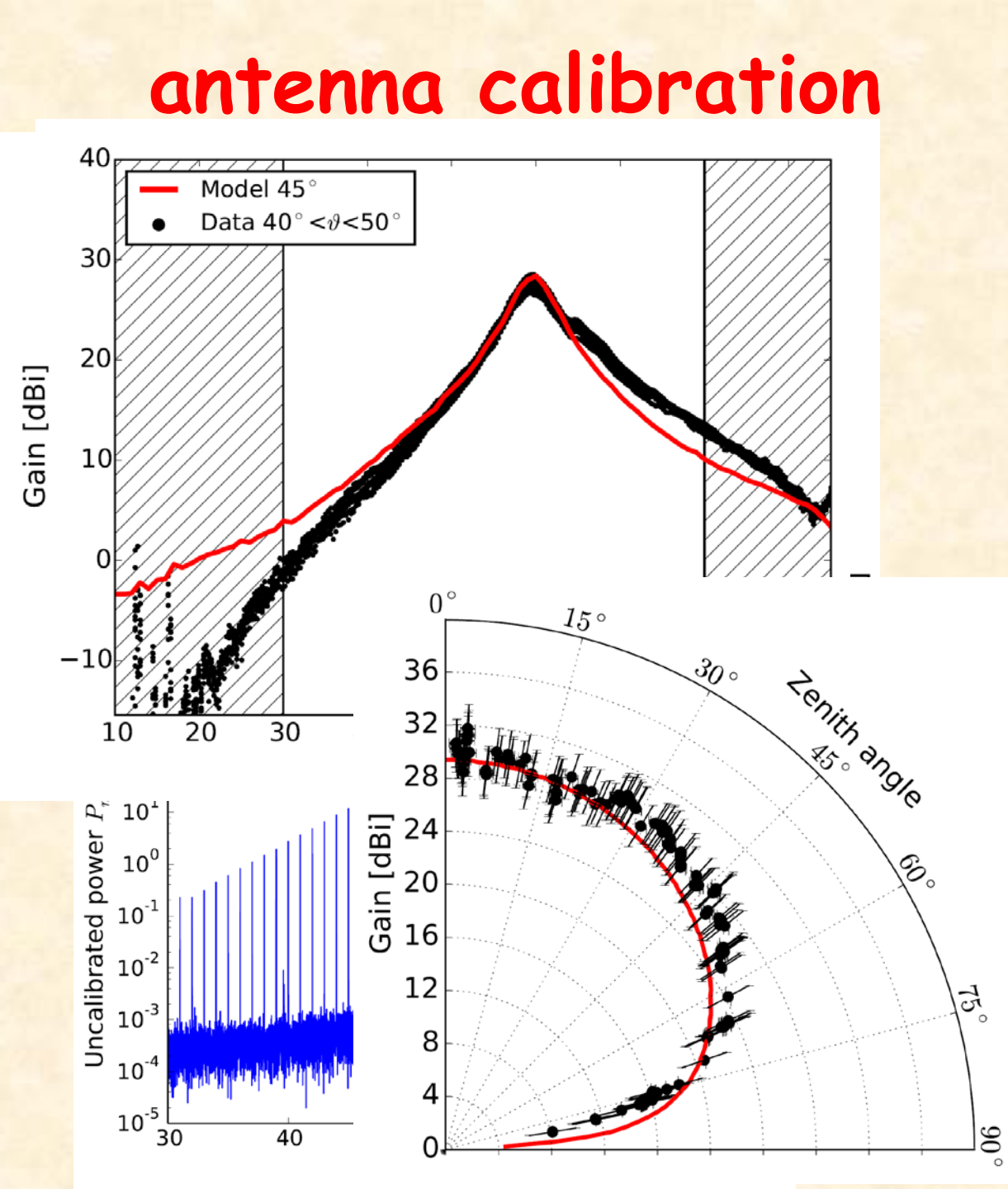
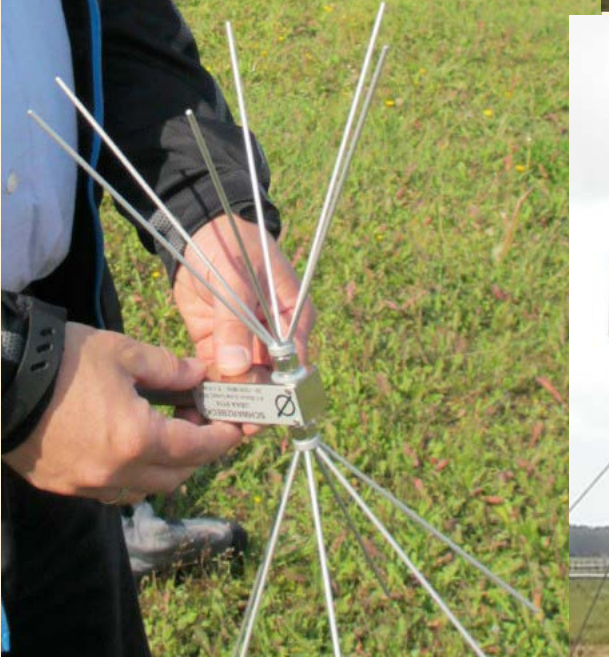
Gia Trinh



## Reason for fair-weather circular polarization:

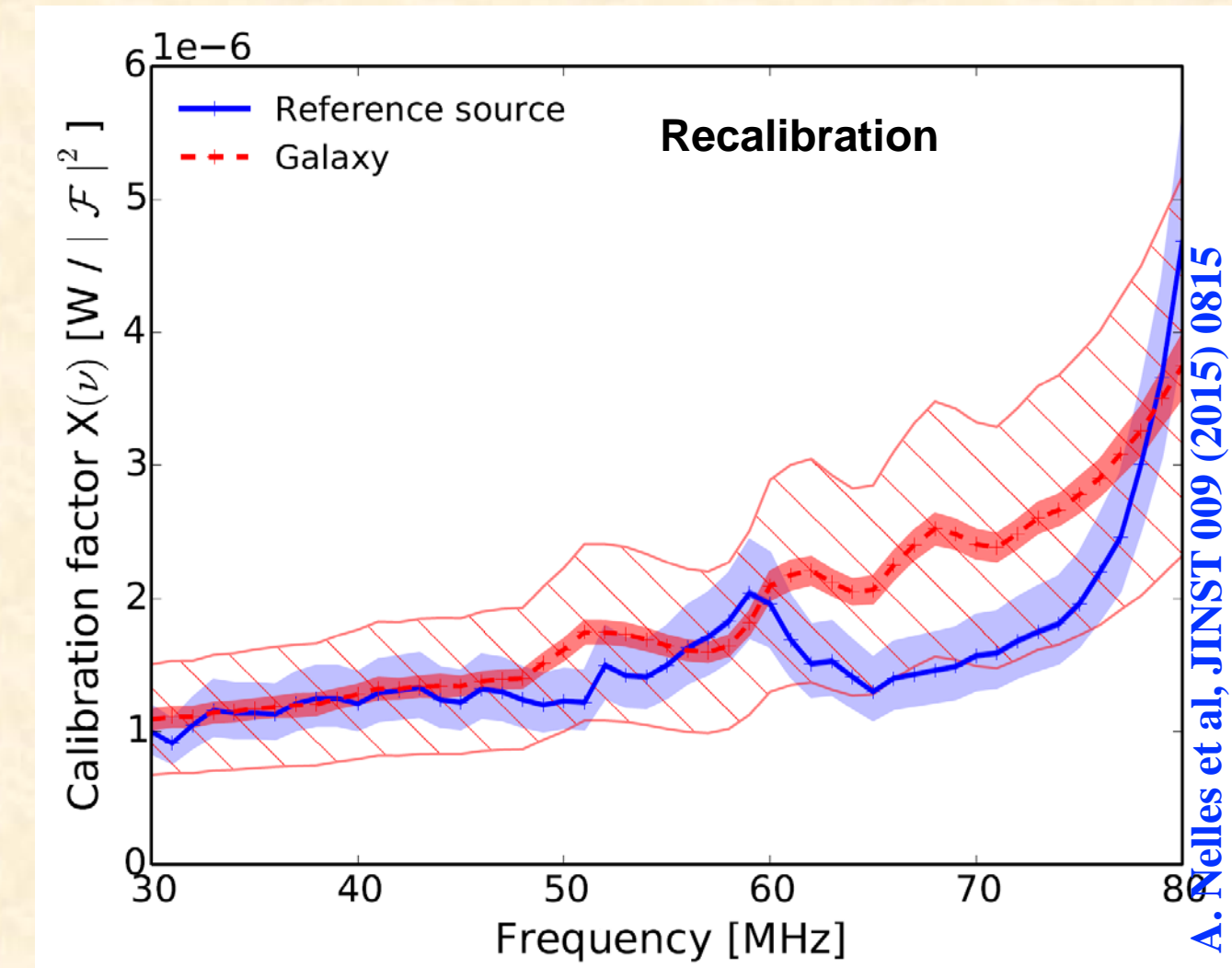
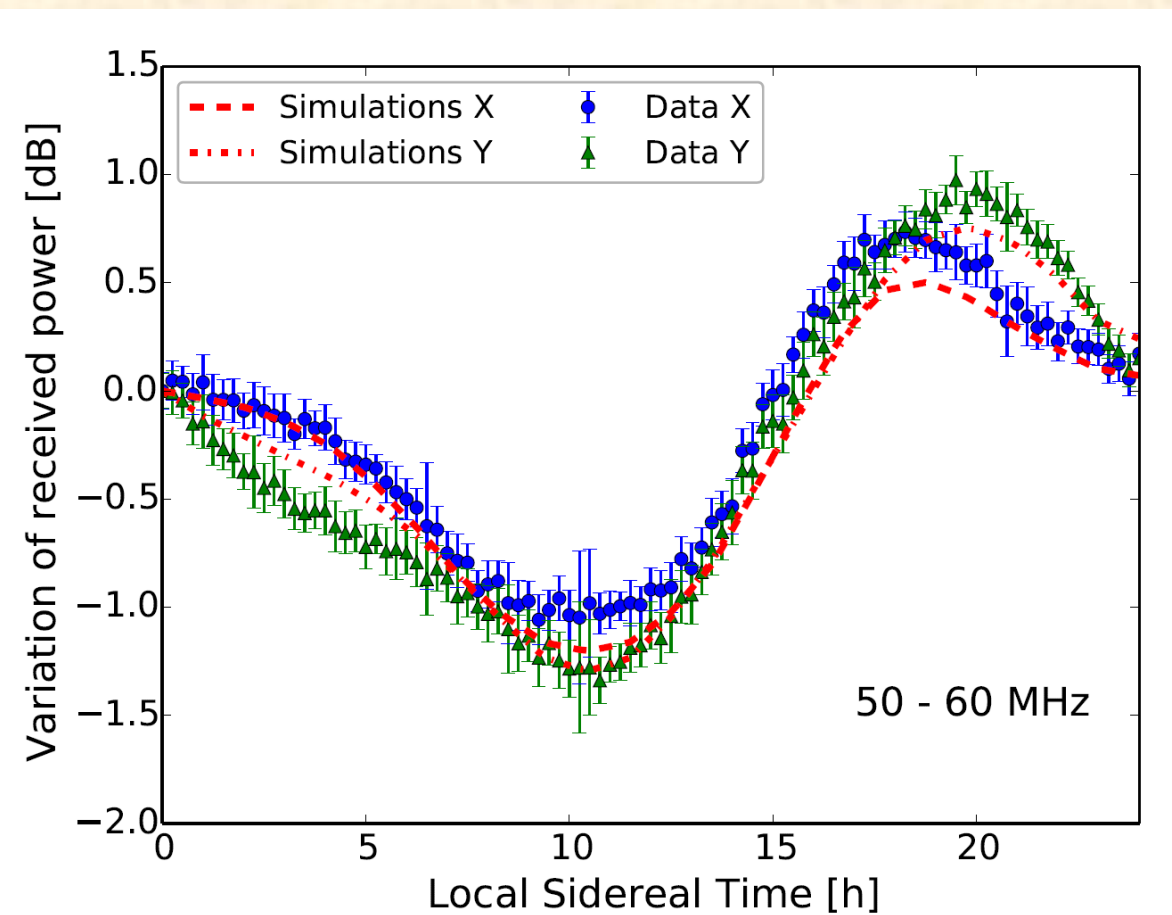
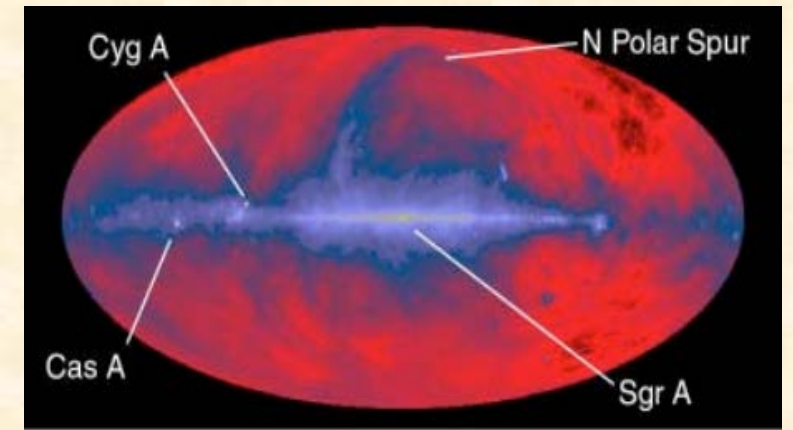
**Transverse current is 1ns ahead of Charge excess pulse**



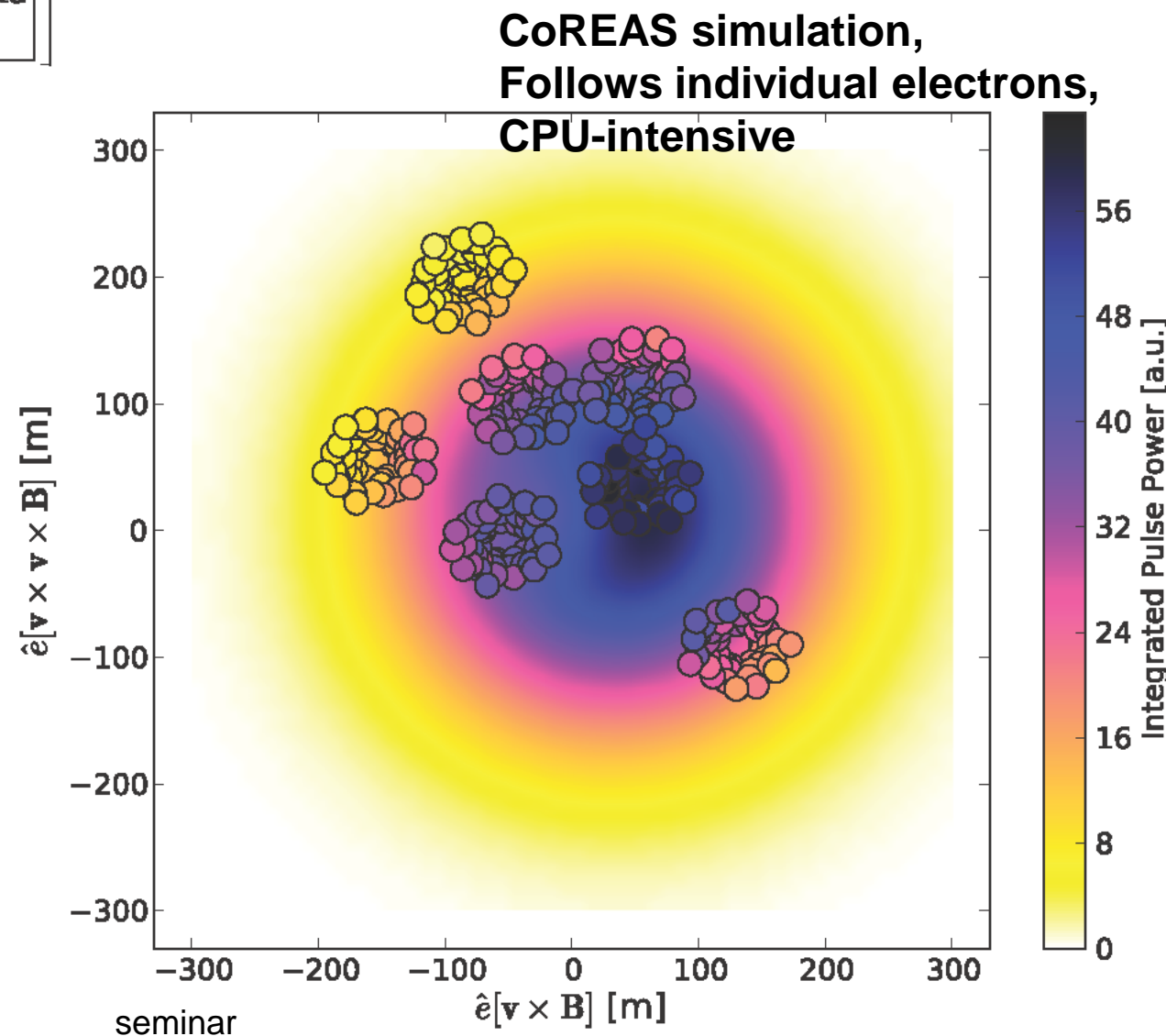
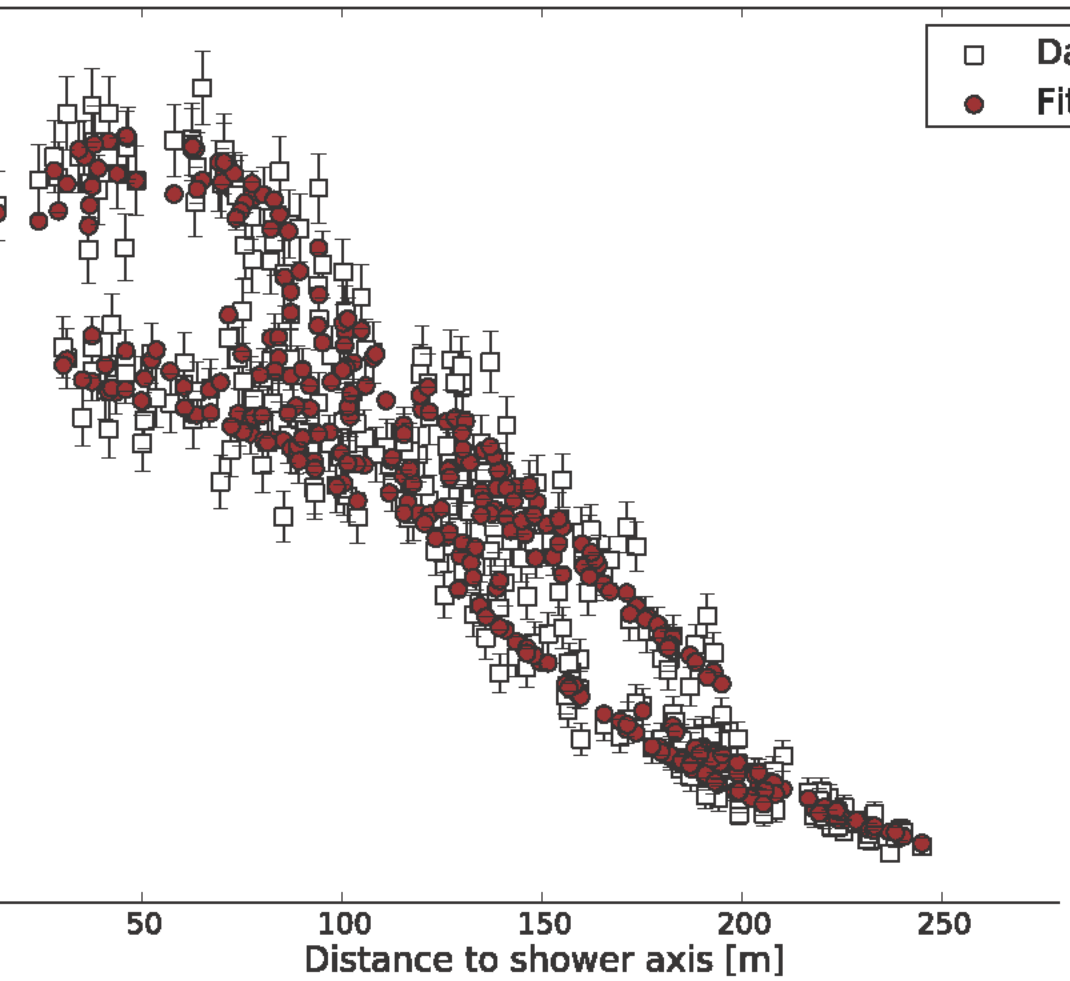


# Gain of complete signal chain

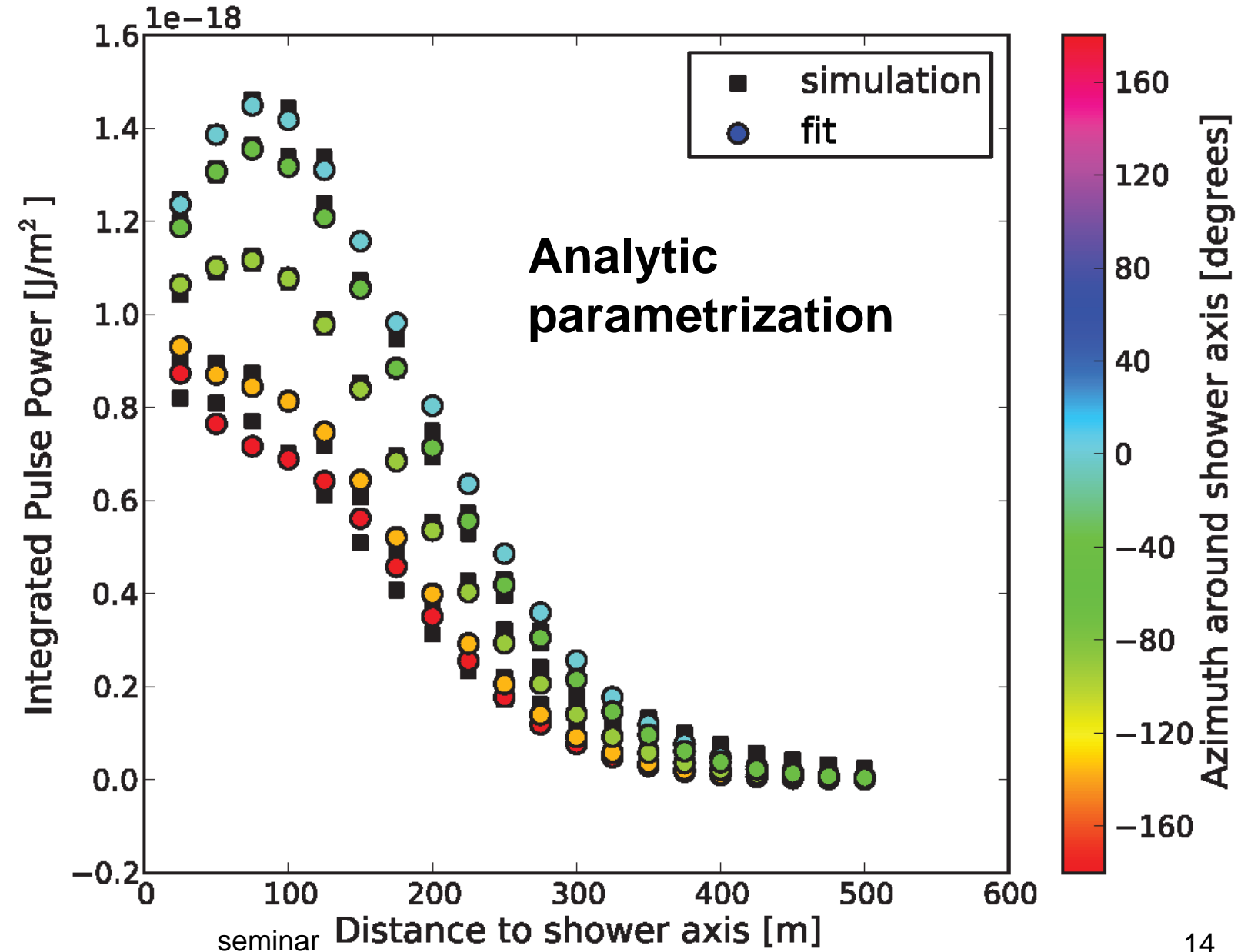
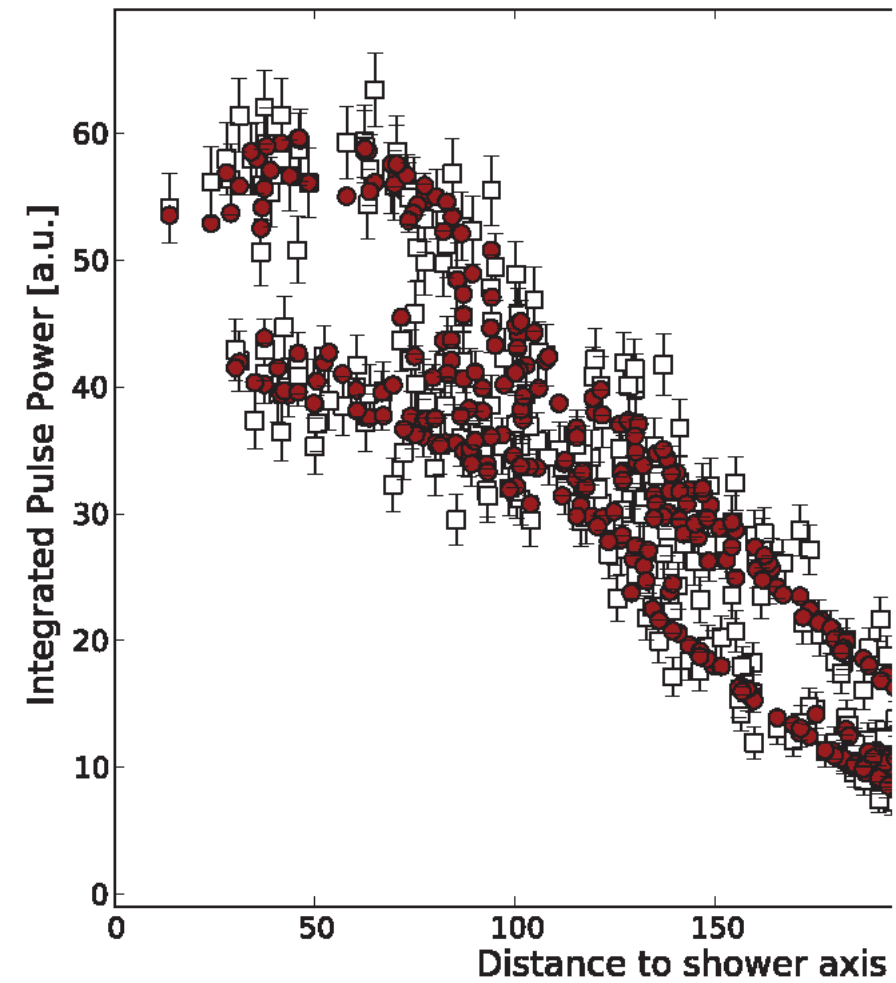
## Galactic background



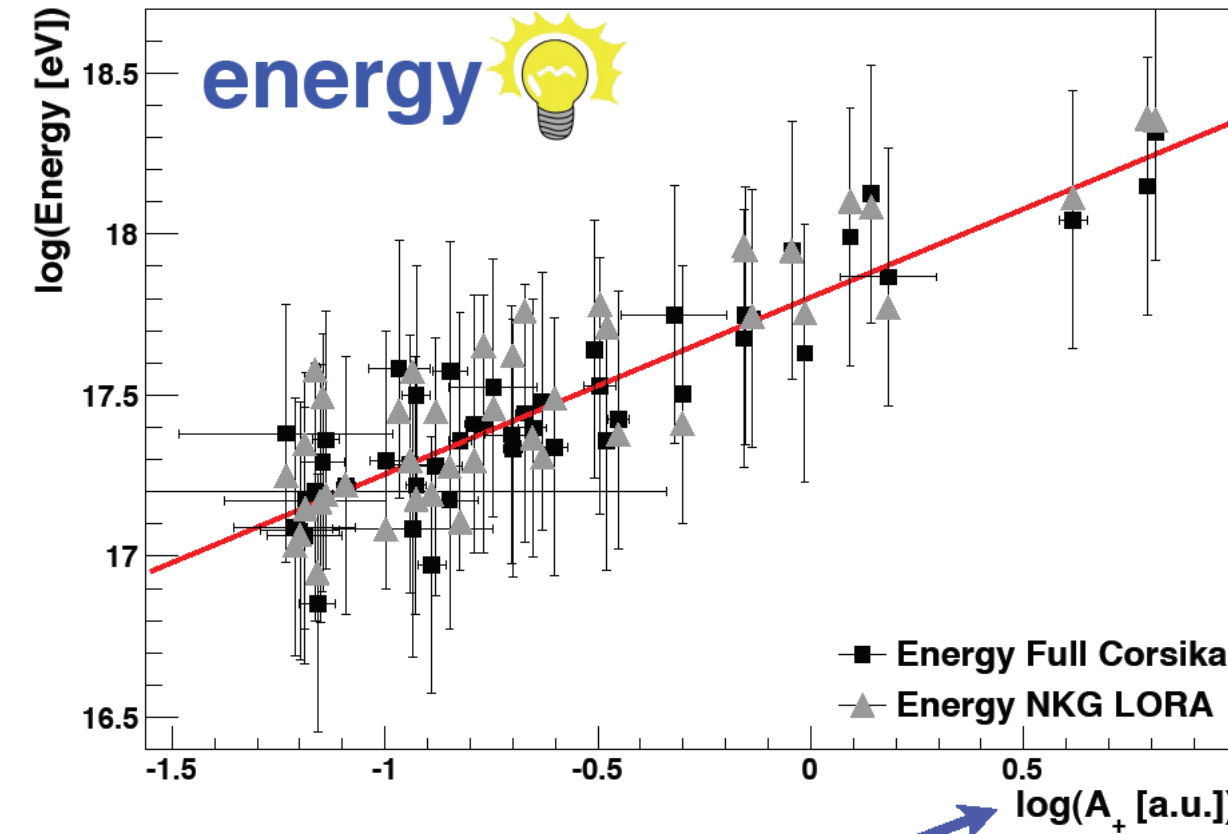
# Lateral distribution of radio signals as measured by LOFAR



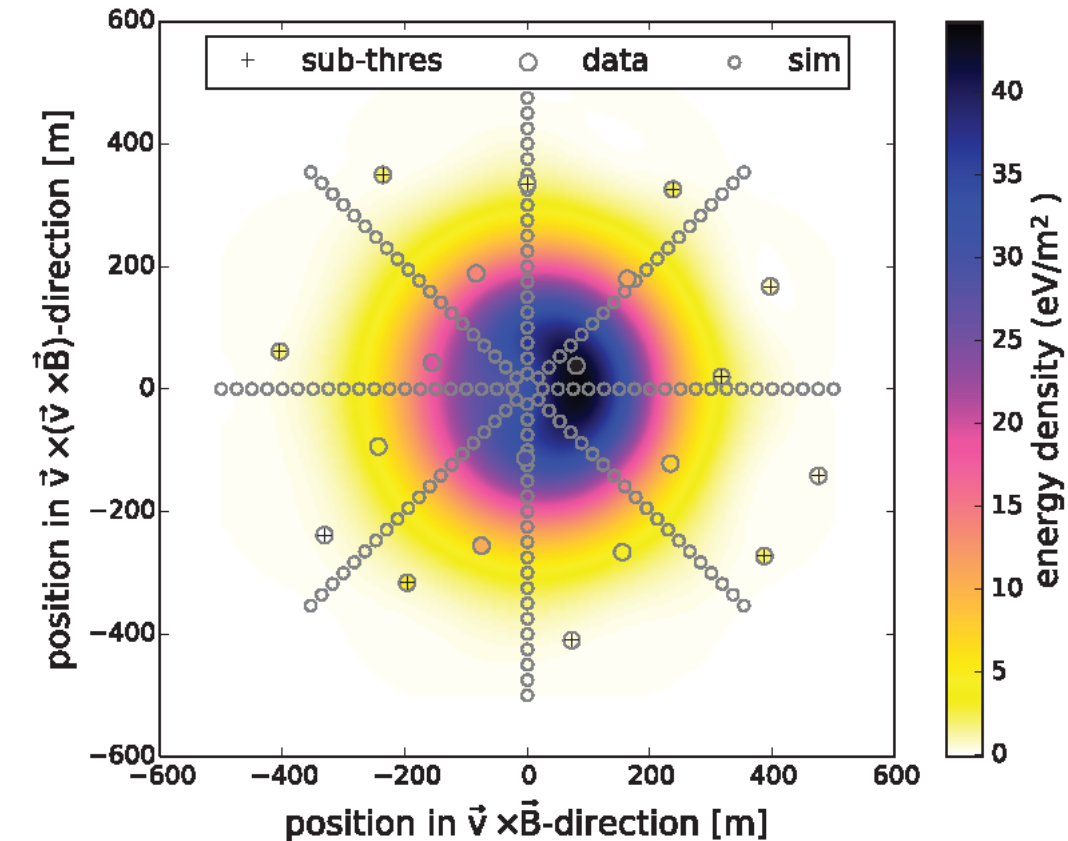
# Lateral distribution of radio signals



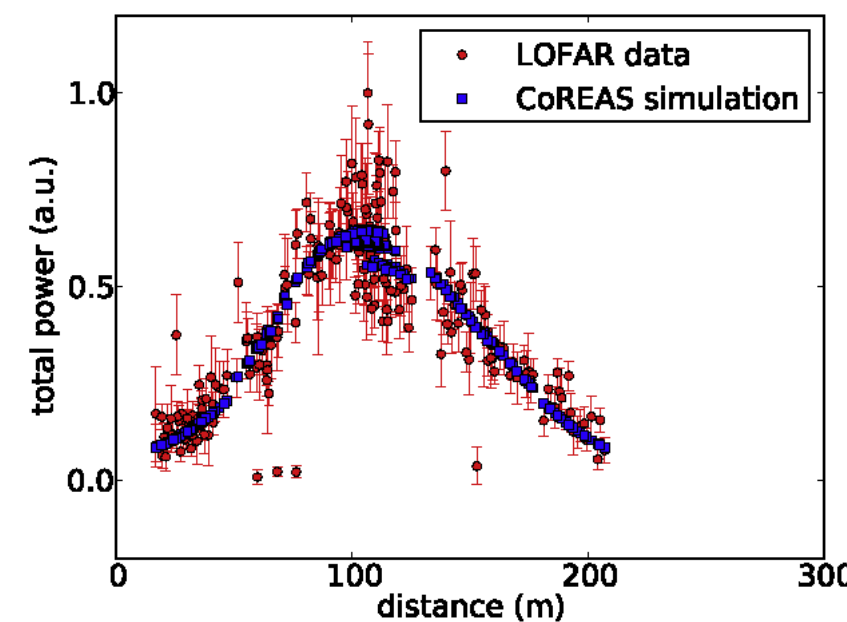
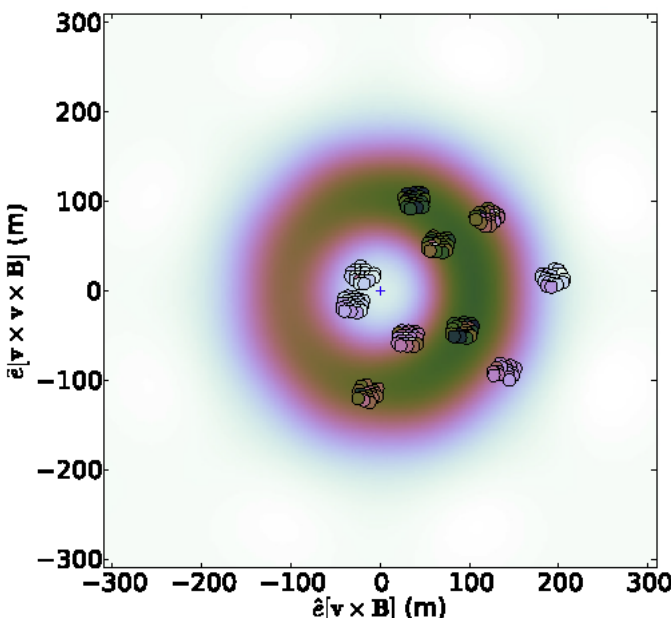
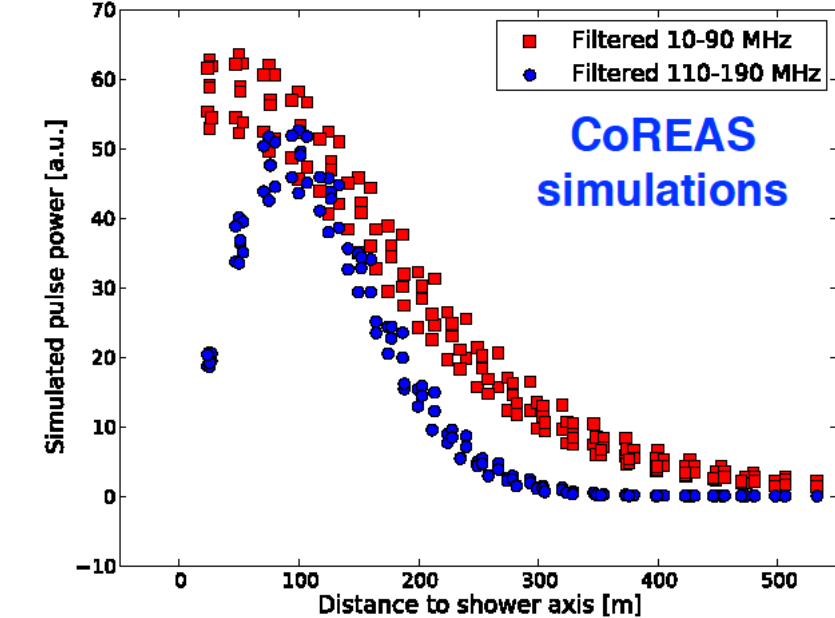
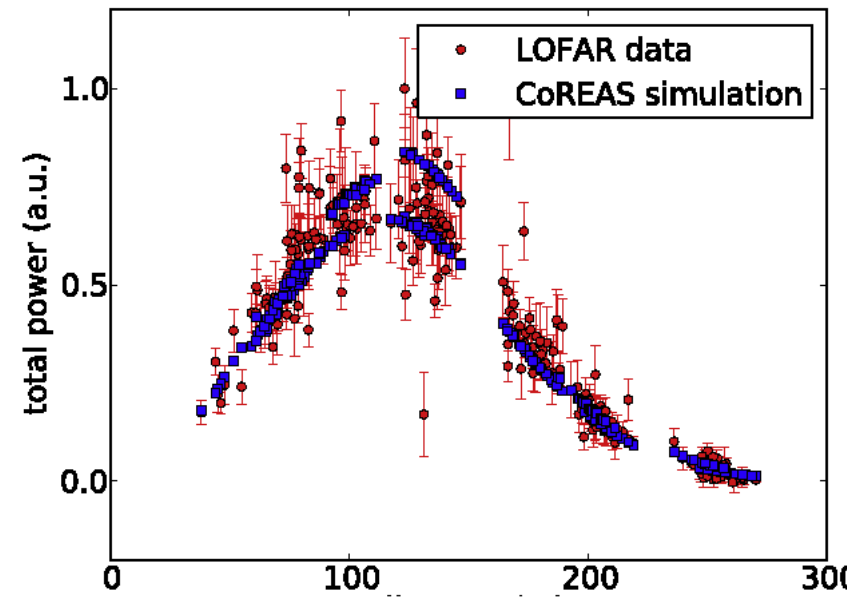
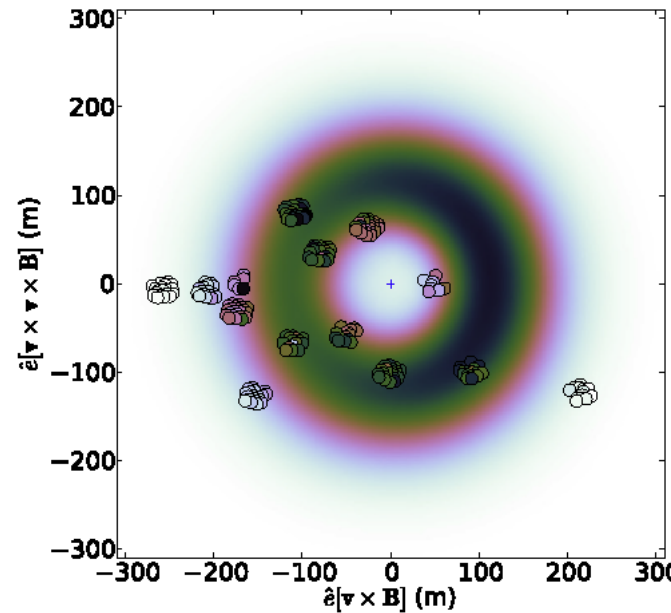
# Properties of primary particle



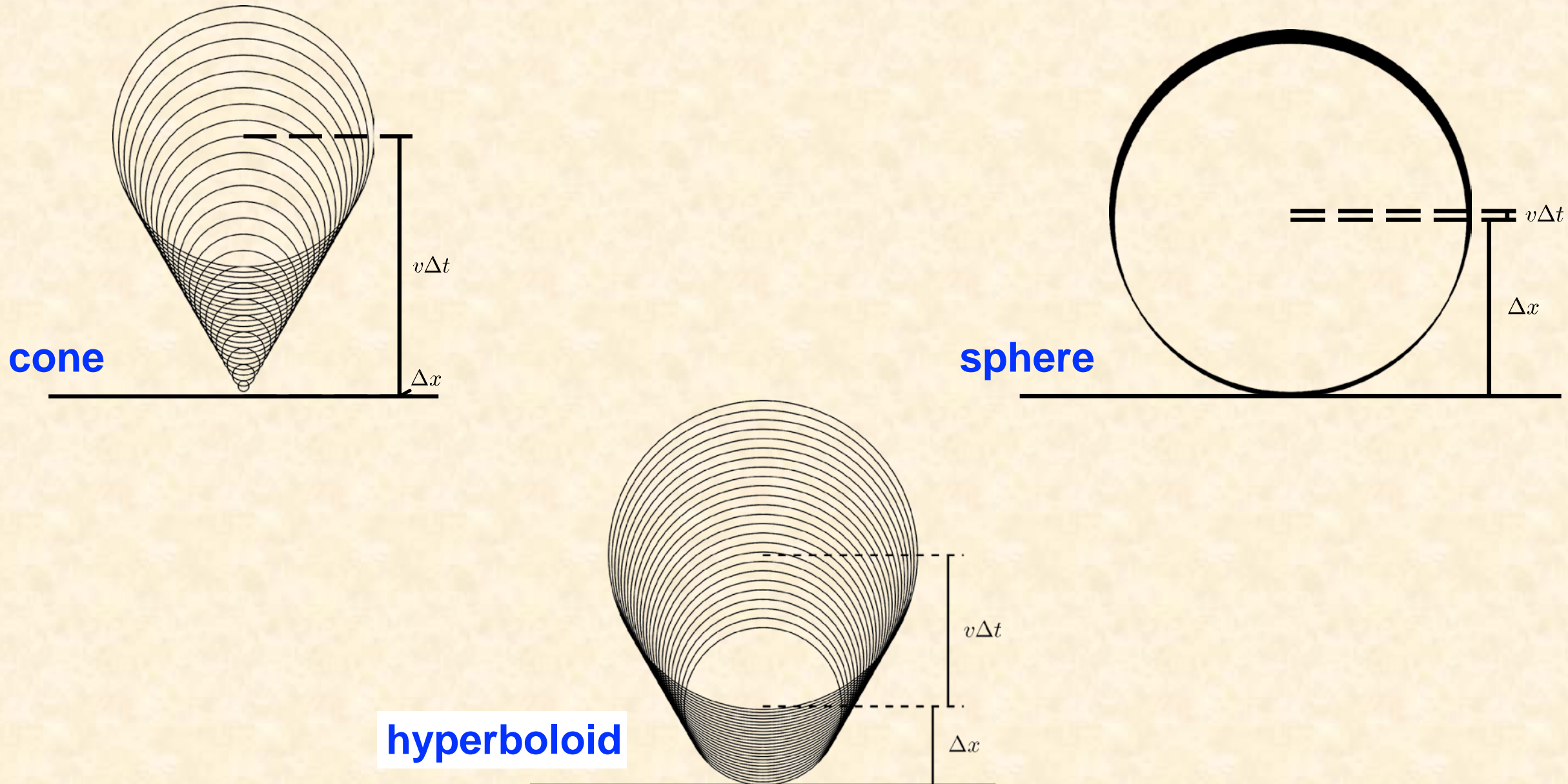
$$P(x', y') = A_+ \cdot \exp\left(\frac{-[(x' - X_+)^2 + (y' - Y_+)^2]}{\sigma_+^2}\right) - A_- \cdot \exp\left(\frac{-[(x' - X_-)^2 + (y' - Y_-)^2]}{\sigma_-^2}\right) + O$$



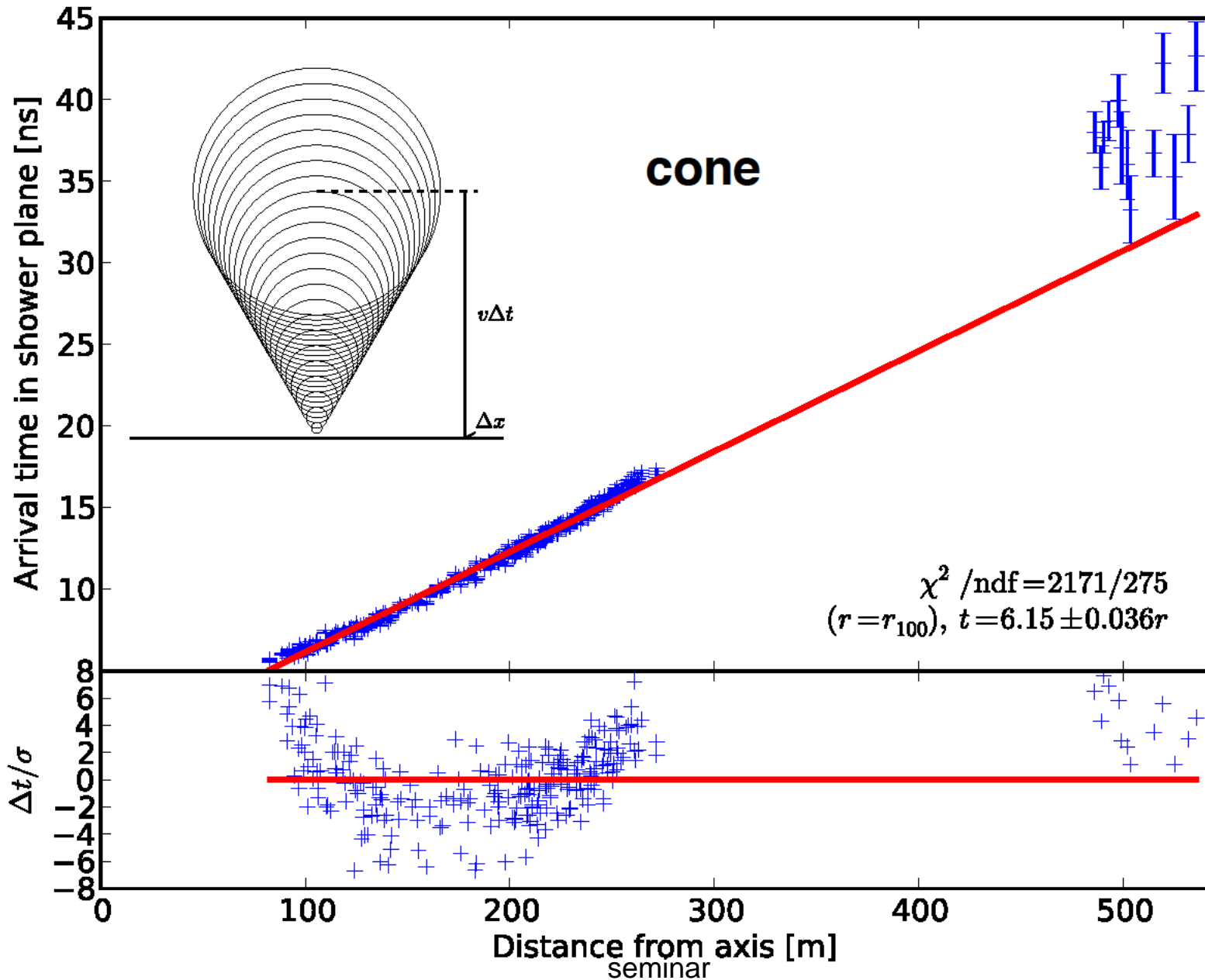
# Measuring Cherenkov Rings 110 - 190 MHz



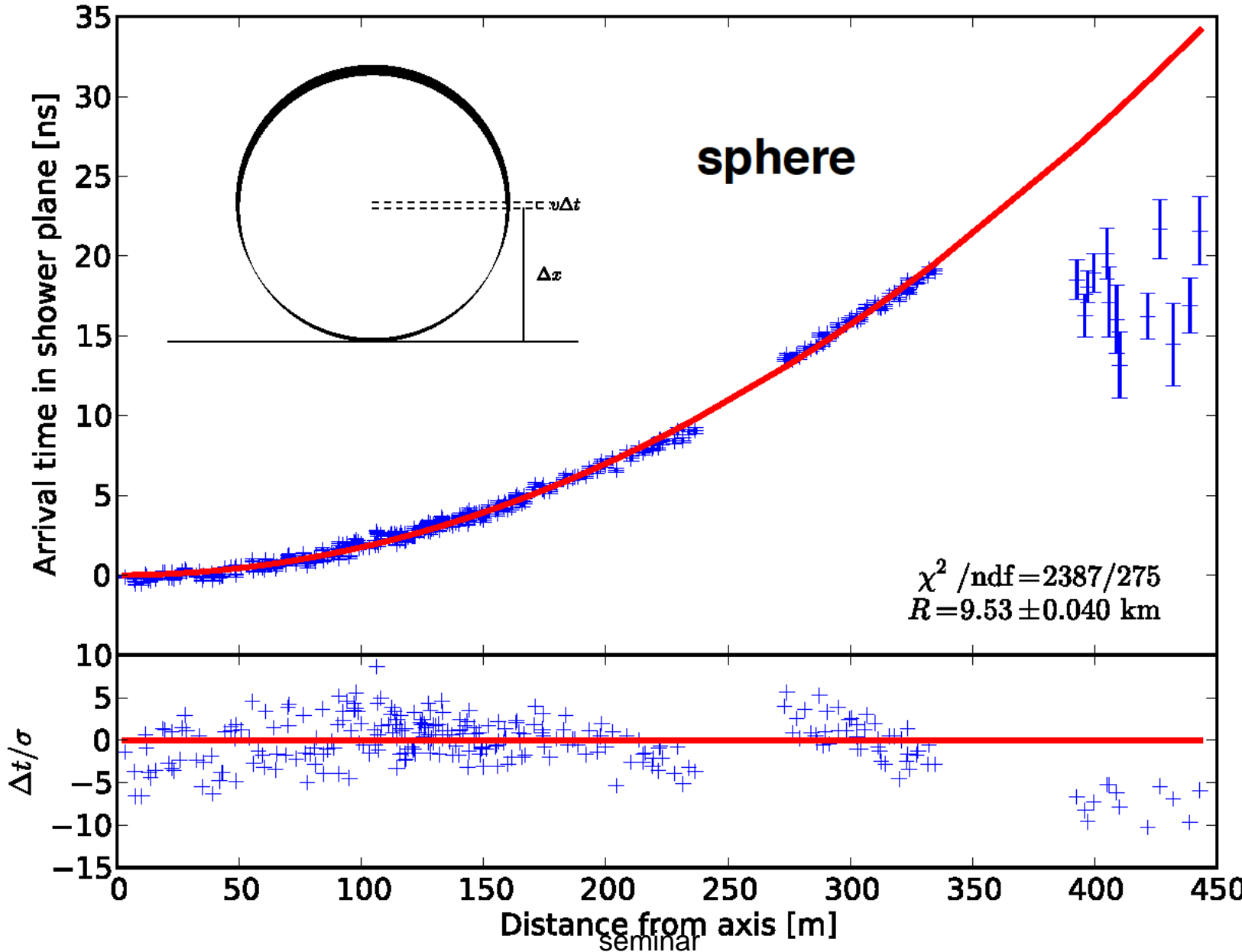
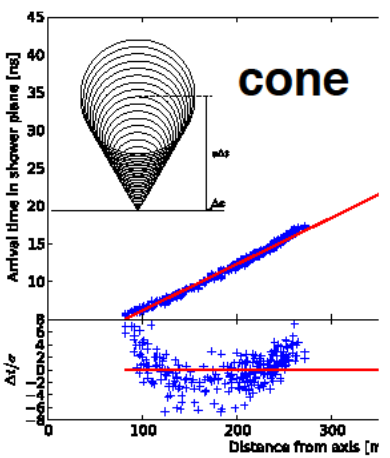
# Shape of the Shower Front



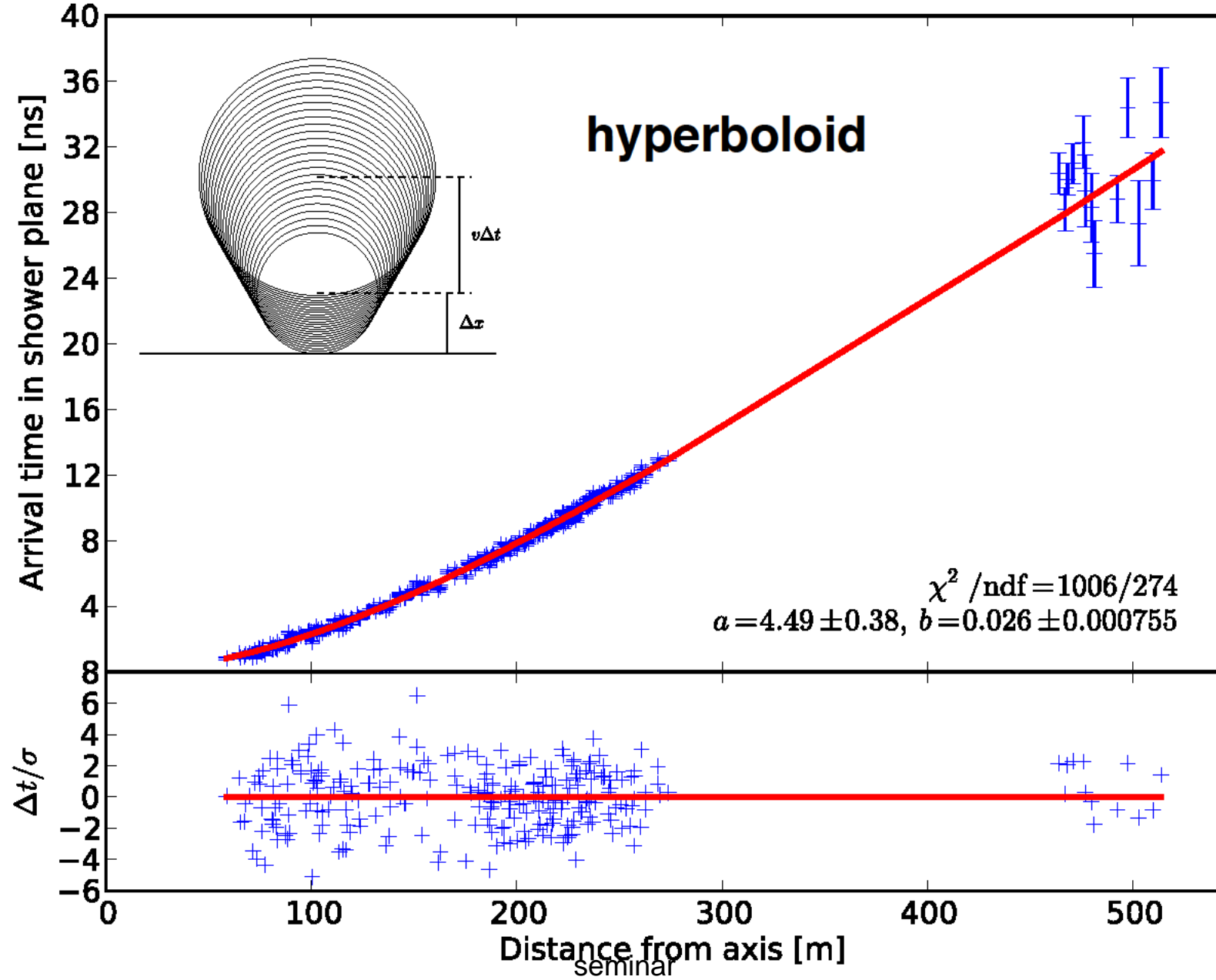
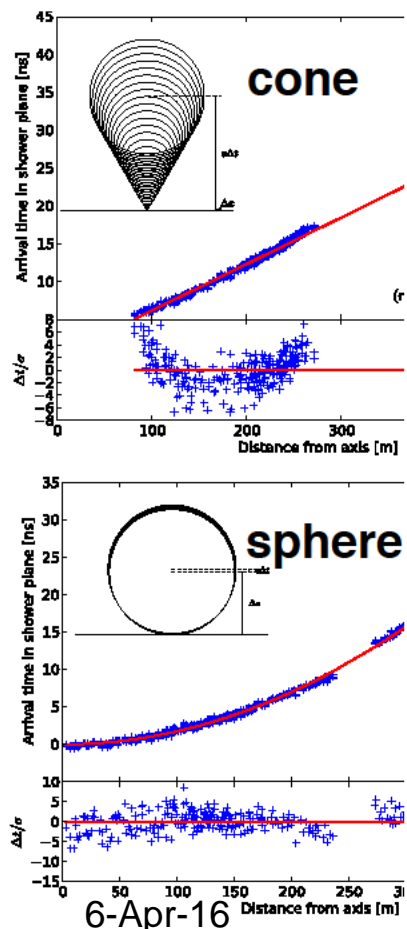
# Arrival time of radio signals



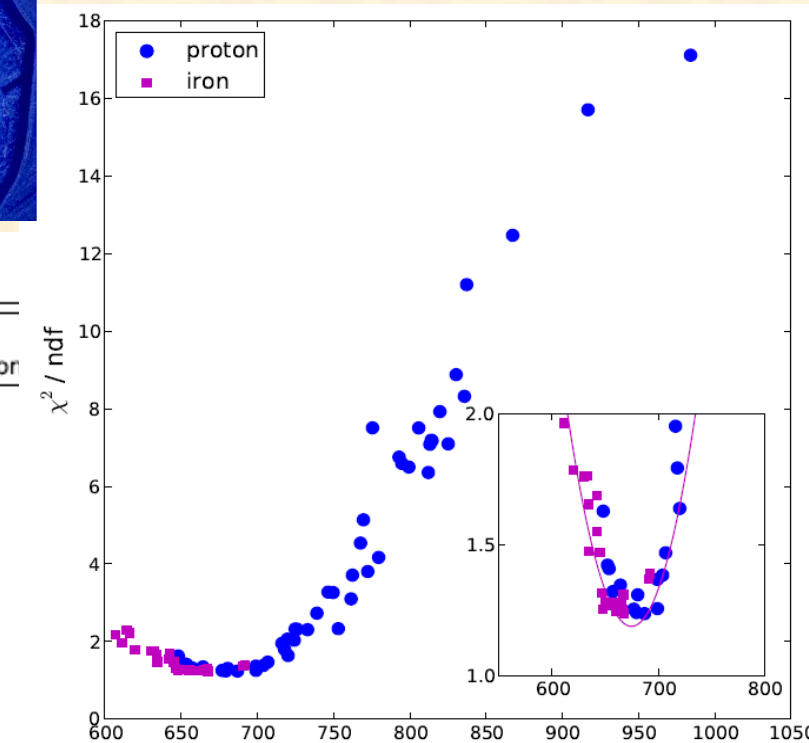
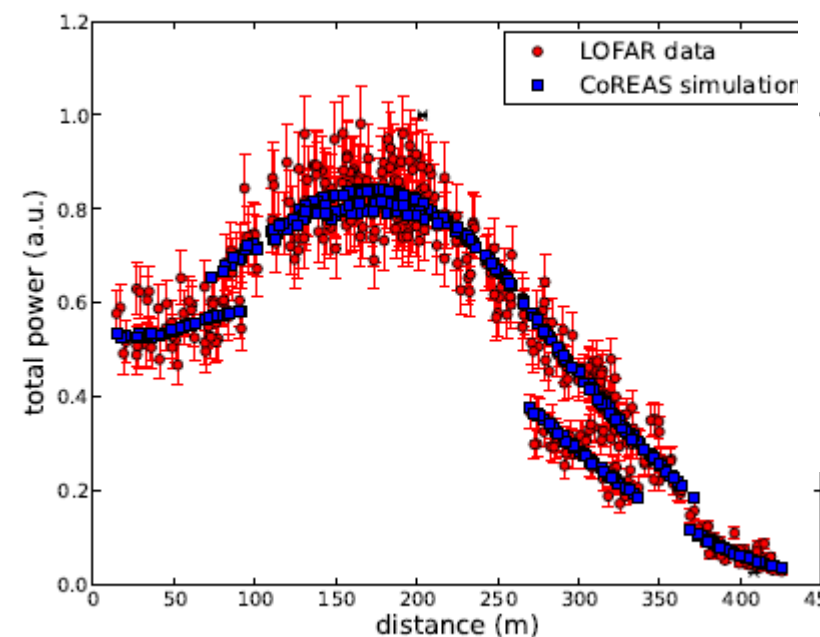
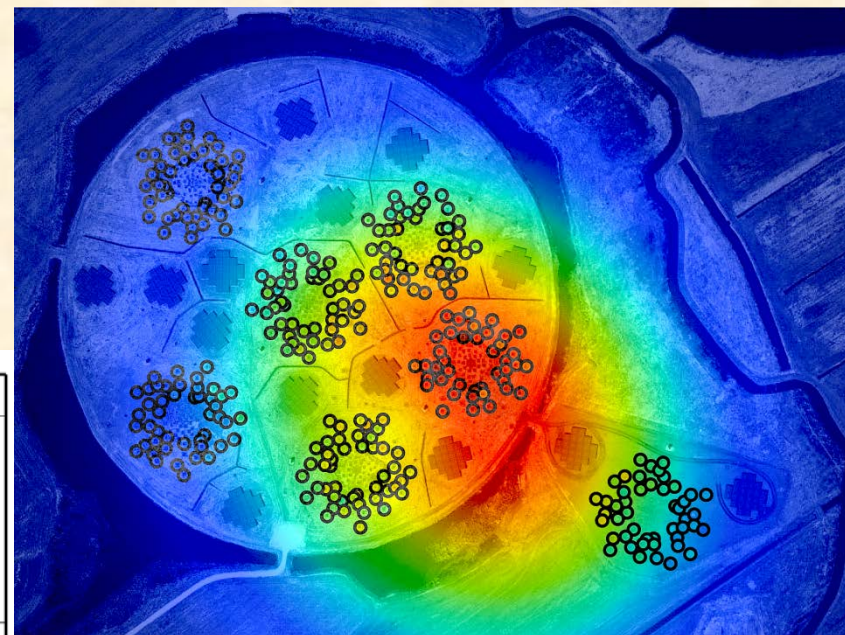
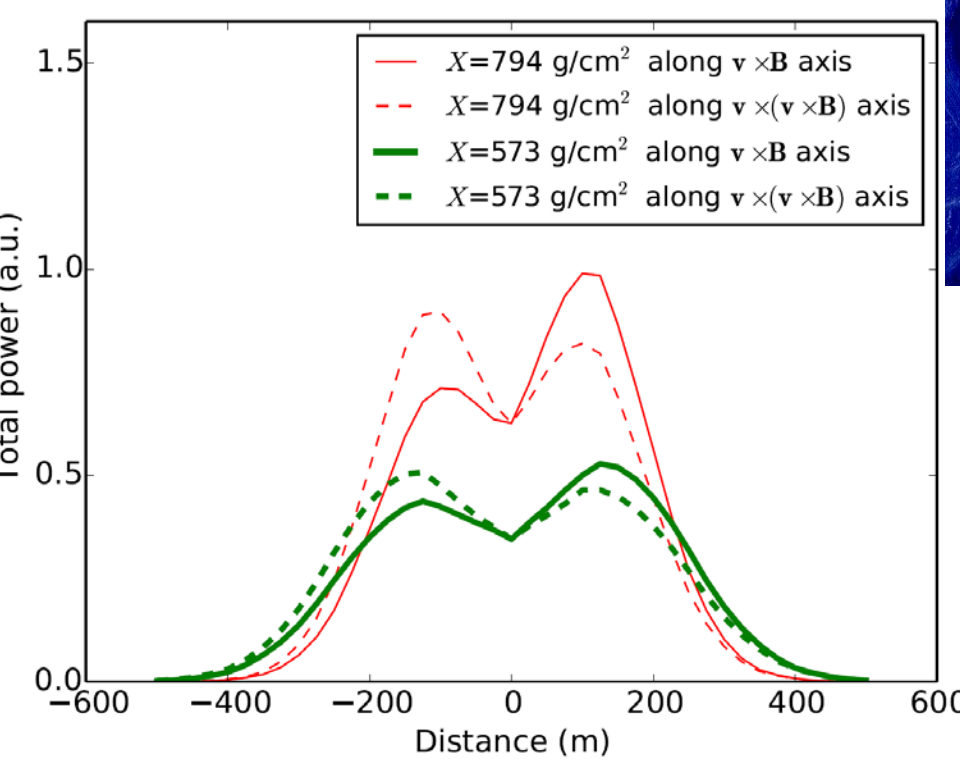
# Arrival time of radio signals



# Arrival time of radio signals



# LOFAR CR-radio detection



$X_{\max}$  resolution = 20 g/cm<sup>2</sup>

# Depth of the shower maximum

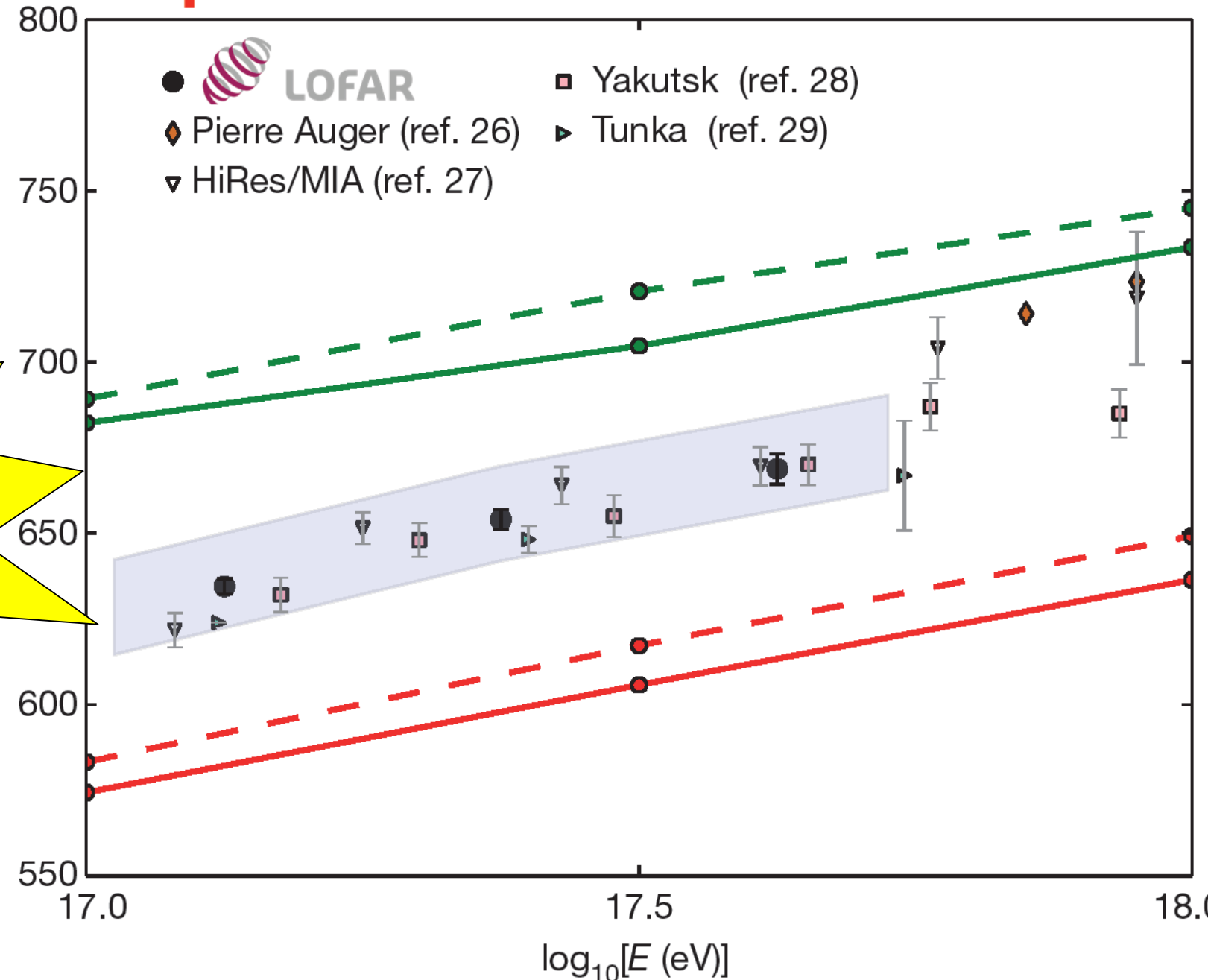
## A large light-mass component of cosmic rays at $10^{17}$ – $10^{17.5}$ electronvolts from radio observations

S. Buitink<sup>1,2</sup>, A. Corstanje<sup>3</sup>, H. Falcke<sup>2,3,4,5</sup>, J. R. Hörandel<sup>2,4</sup>, T. Huege<sup>6</sup>, A. Nelles<sup>2,7</sup>, J. P. Rachen<sup>2</sup>, L. Rossetto<sup>2</sup>, P. Schellart<sup>2</sup>, O. Scholten<sup>8,9</sup>, S. ter Veen<sup>3</sup>, S. Thoudam<sup>2</sup>, T. N. G. Trinh<sup>8</sup>, J. Anderson<sup>10</sup>, A. Asgekar<sup>3,11</sup>, I. M. Avruch<sup>12,13</sup>, M. E. Bell<sup>14</sup>, M. J. Bentum<sup>14,15</sup>, G. Bernardi<sup>16,17</sup>, P. Best<sup>18</sup>, A. Bonafede<sup>16</sup>, F. Breitling<sup>19</sup>, J. W. Broderick<sup>20</sup>, W. N. Brouw<sup>1,13</sup>, M. Brüggen<sup>19</sup>, H. R. Butcher<sup>21</sup>, D. Carbone<sup>23</sup>, B. Giard<sup>24</sup>, J. E. Conway<sup>25</sup>, F. de Gasperin<sup>19</sup>, E. de Geus<sup>3,26</sup>, A. Deller<sup>3</sup>, R.-J. Dettmar<sup>27</sup>, G. van Diepen<sup>3</sup>, S. Duschl<sup>3</sup>, J. Eisloffel<sup>28</sup>, D. Engels<sup>29</sup>, J. E. Enriquez<sup>3</sup>, R. A. Fallows<sup>3</sup>, R. Fender<sup>30</sup>, C. Ferraria<sup>1</sup>, W. Frieswijk<sup>3</sup>, M. A. Garrett<sup>32</sup>, J. M. Grießmeier<sup>33,34</sup>, A. W. Gunst<sup>3</sup>, M. P. van Haarlem<sup>3</sup>, T. E. Hassall<sup>21</sup>, G. Heald<sup>1,13</sup>, J. W. T. Hessels<sup>3,23</sup>, M. Hoeft<sup>31</sup>, A. Horneffer<sup>3</sup>, M. Iacobelli<sup>3</sup>, H. Intema<sup>32,35</sup>, E. Juette<sup>27</sup>, A. Karastergiou<sup>30</sup>, V. I. Konstantinov<sup>3,36</sup>, M. Kramer<sup>3,27</sup>, M. Kuniyoshi<sup>32</sup>, G. Kuper<sup>3</sup>, J. van Leeuwen<sup>3,23</sup>, G. M. Loose<sup>3</sup>, P. Maaß<sup>20</sup>, C. Mann<sup>20</sup>, S. Markoff<sup>3</sup>, R. McFadden<sup>3</sup>, D. McKay-Bukowski<sup>39,40</sup>, J. P. McKean<sup>3,12</sup>, M. Mevius<sup>3,13</sup>, D. Mulcahy<sup>21</sup>, H. Munk<sup>3</sup>, M. I. Norden<sup>3</sup>, E. Orru<sup>3</sup>, H. Paas<sup>41</sup>, M. Pandey-Pommier<sup>42</sup>, V. N. Pandey<sup>3</sup>, M. Pietka<sup>30</sup>, R. Pizzo<sup>3</sup>, A. G. Polatidis<sup>3</sup>, W. Reich<sup>3</sup>, H. J. A. Röttgering<sup>22</sup>, A. M. M. Scaife<sup>3</sup>, D. I. Schwarz<sup>43</sup>, M. Seryak<sup>30</sup>, J. Sluman<sup>3</sup>, O. Smirnov<sup>37,44</sup>, B. W. Stappers<sup>3</sup>, M. Steinmetz<sup>30</sup>, A. Stewart<sup>30</sup>, J. Swinbank<sup>23,45</sup>, M. Tagger<sup>33</sup>, Y. Tang<sup>3</sup>, C. Tasse<sup>34,46</sup>, M. C. Toribio<sup>3,32</sup>, R. Vermeulen<sup>3</sup>, C. Vocks<sup>30</sup>, C. Vogt<sup>3</sup>, R. J. van Weeren<sup>3</sup>, R. A. M. J. Wijers<sup>23</sup>, S. J. Wijnholds<sup>3</sup>, M. W. Wise<sup>3,23</sup>, O. Wucknitz<sup>3</sup>, S. Yatawatta<sup>3</sup>, P. Zarka<sup>47</sup> & J. A. Zensus<sup>3</sup>

Cosmic rays are the highest-energy particles found in nature. Measurements of the mass composition of cosmic rays with energies of  $10^{17}$ – $10^{18}$  electronvolts are essential to understanding whether they have galactic or extragalactic sources. It has also been proposed that the astrophysical neutrino signal<sup>1</sup> comes from accelerators capable of producing cosmic rays at these energies<sup>2</sup>. Cosmic rays initiate air showers—cascades of secondary particles in the atmosphere—and their masses can be inferred from measurements of the atmospheric depth of the shower. The depth of the air shower when it contains the highest energy particles, or the composition of shower particles reaching the ground, are current measurements<sup>3</sup> with either high uncertainty<sup>4</sup> or a low signal-to-noise ratio and a high energy threshold. Radio detection is a rapidly developing technique<sup>5</sup> for determining the mass composition of cosmic rays with a duty cycle of, in principle, nearly 100 percent. This is generated by the separation of relativistic electrons along the magnetic field and a negative charge excess in front<sup>6,12</sup>. Here we report radio measurements of the depth of the air shower maximum ( $X_{\max}$ ) with an uncertainty of 16 grams per square centimetre.

## Nature

published  
in nature



# Papers 2015 & 16

A. Bonardi, S. Buitink, A. Corstanje, J.E. Enriquez, H. Falcke,  
J.R. Hörandel, T. Karskens, M. Krause, P. Mitra, K. Mulrey, A. Nelles,  
J.P. Rachen, L. Rossetto, P. Schellart, O. Scholten, S. Thoudam, T.N.G. Trinh , S. ter Veen, T. Winchen



- 1 - Calibrating the absolute amplitude scale for air showers measured at LOFAR,  
A. Nelles et al., *JINST* 009 (2015) 0815
- 2 - Probing atmospheric electric fields in thunderstorms through radio emission from cosmic-ray induced air showers  
P. Schellart et al., *Physical Review Letters* 114 (2015) 165001
- 3 - Measuring a Cherenkov ring in the radio emission from air showers at 110 - 190 MHz with LOFAR  
A. Nelles et al., *Astroparticle Physics* 65 (2015) 11
- 4 - The shape of the radio wavefront of extensive air showers as measured with LOFAR  
A. Corstanje et al., *Astroparticle Physics* 61 (2015) 22
- 5 - A parameterization for the radio emission of air showers as predicted by CoREAS simulations and applied to LOFAR measurements  
A. Nelles et al., *Astroparticle Physics* 60 (2015) 13
- 6 - The radio emission pattern of air showers as measured with LOFAR - a tool for the reconstruction of the energy and the shower maximum  
A. Nelles et al., *Journal of Cosmology and Astroparticle Physcis* 05 (2015) 018
- 7 - Influence of atmospheric electric fields on the radio emission from extensive air showers  
T.N.G. Trinh et al., *Physical Review D* 93 (2016) 023003
- 8 - Measurement of the cosmic-ray energy spectrum above 10<sup>16</sup> eV with the LOFAR Radboud Air Shower Array,  
S. Thoudam et al., *Astroparticle Physics* 73 (2016) 34
- 9 - Radio detections of cosmic rays reveal a strong light mass component at 10<sup>17</sup> - 10<sup>17.5</sup> eV  
S. Buitink et al., *Nature* 531 (2016), 70-73
- 10 - Timing calibration and spectral cleaning of LOFAR time series data  
A. Corstanje et al., *Astronomy & Astrophysics*, accepted, arXiv:1603.08354

# A very long title